S Labò, C Passoni, A Marini, A Belleri. 2020. "Design of diagrid exoskeletons for the retrofit of existing RC buildings". Engineering Structures, Vol. 220, pp. 1-20. DOI: 10.1016/j.engstruct.2020.110899

Publisher's version at: https://doi.org/10.1016/j.engstruct.2020.110899

Design of diagrid exoskeletons for the retrofit of existing RC buildings

Simone Labò, Chiara Passoni, Alessandra Marini, Andrea Belleri

Abstract

The pursuit of a sustainable society requires an extensive intervention on the existing buildings, which are responsible for the major share of greenhouse gas (GHG) emissions. In addition, such constructions have exhausted their nominal structural service life and are vulnerable to seismic hazard. In such a scenario, new integrated retrofit techniques have been proposed to foster the holistic and sustainable renovation of the European obsolete building stock, thereby boosting the current renovation rate.

In this paper, diagrids are proposed as structural exoskeletons for the renovation of existing reinforced concrete (RC) buildings. The diagrid system is an inclined structural grid withstanding both vertical and horizontal loads to which a building is subjected. Such a system was initially proposed and is usually adopted in tall new buildings with the aim of creating structures with strong architectural identity, without vertical columns. Diagrids are suitable solutions for the integrated renovation (energy, architecture and structure) of existing buildings, and they may be applied from outside to avoid the occupants' relocation. They may be assembled in different steps over an extended period of time by adopting an incremental rehabilitation strategy, thereby increasing the economic sustainability of the interventions; finally, they may be designed in full compliance with the principles of Life Cycle Thinking.

In this paper, two methods for the design of elastic diagrids as retrofit intervention are proposed. The first method is an analytical design method which can be regarded as the extension of previous studies on diagrid systems for tall new buildings. The second method entails the definition of design spectra from which both stiffness and strength of the diagrid exoskeleton can be obtained. The latter is obtained from sensitivity analyses carried out on a simplified SDOF system and it stems as the extension of existing procedures for the design of bracing systems. Both methods are then applied for the design of the structural retrofit of a RC building typical of the post-WWII European building stock. Theoretical results have been compared with results obtained with nonlinear time history analyses, showing the effectiveness of the proposed design methods.

1. Introduction

The building sector is acknowledged as the most impacting sector worldwide because of the obsolescence of the existing building stock, its energy inefficiency, and its inherent vulnerability to natural hazards such as earthquakes. The deep renovation of the existing building heritage is thus now acknowledged as a priority to foster sustainability throughout Europe.

Despite the multiple needs of the existing buildings, the retrofit solutions are still conceived in an uncoupled manner and designed by addressing very sectorial codes, targeting one single topic at the time (either energy efficiency, acoustic insulation, structural rehabilitation). As a consequence of the current practice, an upgrade of the sole energy performances may leave the building structurally unsafe; conversely, a structural retrofit, usually carried out in emergency situation, may result in an environmentally unsustainable intervention, despite being fully compliant with the current structural building codes. A new and integrated approach to the building renovation is thus required, and new techniques and solution sets must be conceived to overcome all the deficiencies of the existing buildings, thereby pursuing sustainability, safety, and resilience at the same time [1]. In this scenario, the paper's original contribution relies on the proposal of diagrid exoskeletons as a novel technique to be adopted in the deep integrated renovation of existing RC buildings.

Diagrids were first introduced as bearing structures for tall buildings. The term *diagrid* derives from the union of two terms: "diagonal" and "grid" [2], and refers to a structural system that gains its structural integrity through triangular modules composed by 2 diagonal elements of length L_d and inclination ψ, and 1 horizontal element (*Figure 1*). Diagrids can be regarded as the evolution of the braced tubular structural systems; in diagrids the diagonal components are located along the exterior perimeter of the building in order to optimize the structural behavior by bearing, with the same structural system, both vertical and horizontal loads [3].

In this paper, diagrids are applied as additional exoskeletons for the retrofit of existing RC structures, especially to those constructions erected in the post-WWII, particularly between the 60s and the 80s. These constructions are generally clustered in degraded suburbs and are characterized by anonymous architectural features. The solution does not apply in the case preservation of the façades is required or in the case of listed buildings. For the solution to be feasible, compliance with urban planning restrictions must be assessed.

In this context, diagrids are suitable in the integrated/combined deep renovation projects as they can easily integrate the structural elements for the static and seismic upgrading with the new insulation and architectural layers.

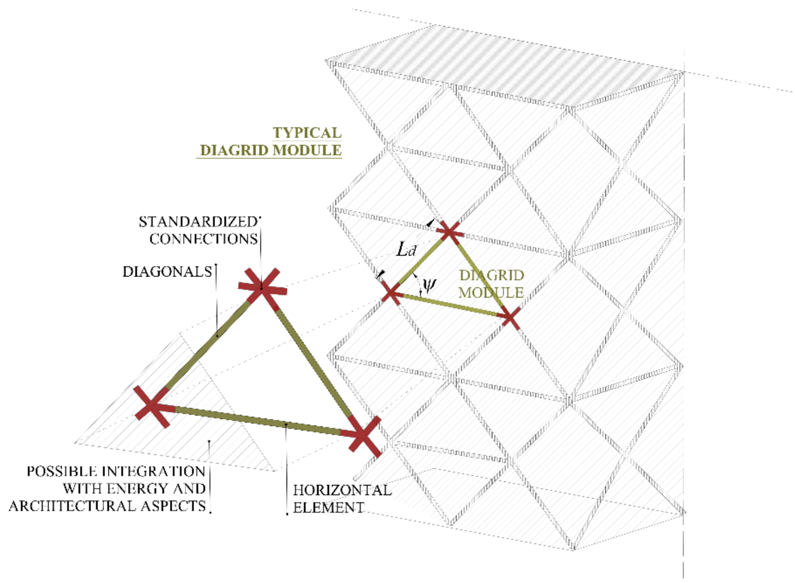

Figure 1 Main components of a diagrid system.

Diagrids may help removing the main barriers that affect the current renovation practice. The extremely low renovation rate of existing buildings (about 1%, [4, 5]) is acknowledged as mostly due to: the need to relocate the occupants, the extended downtime required during the construction works, the high costs of the interventions, and the lack of adequate business models fostering the renovation [4, 6, 7]. In order to overcome these barriers, diagrid exoskeletons can be implemented from the outside of the building, thereby avoiding the occupant's relocation and can implement dry technologies to speed up the construction time. In addition, when the initial costs of the renovation are too demanding, modular diagrids can be developed by adopting an incremental holistic rehabilitation (IHR) strategy [8], which allows to decompose the implementation of the common single step intervention into a series of less impacting retrofit actions to be completed over an extended period of time, often integrating them into ongoing facility maintenance interventions.

As far as environmental sustainability is concerned, diagrids may be conceived by addressing the principles of the Life Cycle Thinking (LCT), which are aimed at minimizing the impacts and costs of the intervention and of the retrofitted building along its whole life cycle [9, 1]. Accordingly, diagrids may implement recyclable/reusable materials, and reparable, easily maintainable, adaptable and fully demountable elements, thus reducing the impacts along the use phase of the building. In addition, standardization and light-prefabrication of its components may guarantee, at the end-of-life, the selective dismantling and reuse or recycle of the components to further reduce the construction waste [9].

In this paper: 1) the simplified static schemes used for diagrid as bearing structures of new tall buildings [3, 10, 11, 12, 13, 14] are revisited and adapted to the requirements for seismic retrofit interventions. The uniform load distribution representing the wind loads in new tall buildings, is substituted by linear and mass proportional load distributions; 2) new simplified design spectra are proposed in order to simplify the design procedure and to derive the optimal diagrid design parameters. The spectra stem as an enhancement of the original research work by Ciampi et al. [15] on bracing systems; novelty relies on a novel approach to the development of the sensitivity analyses; 3) additional design targets and operative choices based on life cycle thinking principles are introduced to increase sustainability and to enable the integrated renovation of the existing building. Considering the extended life cycle timeframe, performance objectives and related design criteria aimed at controlling the behavior of the retrofitted building beyond the design Limit State are introduced; 4) a design procedure for the proportioning of the retrofitting diagrid exoskeleton is proposed and tested by means of non-linear static and dynamic analyses on a reference building resembling a typical post WWII RC construction.

2. Renovation of the existing RC buildings with diagrid exoskeletons: new performance objectives and structural design

The structural design of diagrids as a retrofit solution for existing buildings is a complex process, in which different aspects must be taken into account. The need for a sustainable renovation requires the definition of new design criteria and targets. In addition, the 3D behavior of the diagrid and its discrete nature should be considered.

2.1 New design criteria and performance objectives under a LCT perspective

To foster the sustainability of the renovation process, a new multi-criteria approach [16] aimed at minimizing the environmental, economic, and social impacts of the intervention and of the retrofitted building during the whole Life Cycle should be considered. In this section, an overview of new possible design targets and operative choices for a sustainable and holistic renovation is presented [1].

Design targets are typically expressed in terms of maximum top displacement and inter-story drift, base shear, and maximum floor acceleration so as to prevent collapse and minimize damage on structural and non-structural elements during an earthquake. When a Life Cycle perspective is considered, design targets should be increased in number and reconsidered in their setting values to also minimize impacts during the whole life cycle. Additional operative choices may also be defined to increase the sustainability of the interventions. Possible performance objectives defined under this new perspective are reported in Table 1, together with related design targets and further operative choices.

Design targets for LCT

When sustainable performance objectives are defined and extended to the whole Life Cycle of the retrofitted building, more restrictive design targets may be required with respect to the current practice. As an example, the serviceability of the retrofitted building may be guaranteed also for a lower probability earthquake in order to reduce or even avoid downtime and post-earthquake repair costs [17]. Target displacement, inter-story drift, and floor accelerations necessary to limit the damage into structural and non-structural elements, defined as d_{TOP}, θ_{MAX}, and $a_{floor,max}$, respectively, may thus be guaranteed for the Life Safety Earthquake (LSE, e.g. with a return period equal to 475 years corresponding to a probability of exceedance of 10% in 50 years [18]).

As for social sustainability, retrofit solutions carried out from outside, which limit impacts on the occupants, may be proposed. However, such solutions pose some additional challenges that must be faced by imposing additional design targets. For example, the presence of stiff elements with low ductility (which requires to set a maximum inter-story drift target θ_{MAX}) or the capacity of existing floor diaphragms ($V_{floor,max}$).

As for the structural performance objectives, for LSE, the maximum shear action in existing stiff elements ($V_{staircase,max}$), such as the staircase walls, should be limited to guarantee their operability as egress path after an earthquake; the maximum inter-story drift (θ_{MAX}) could be set as to avoid excessive damage in non-structural elements (NSE such as infills), which are responsible for a high portion of occupants' injuries. In addition, in order to ensure safety and sustainability of the intervention, the behavior of the system for the Collapse Prevention Earthquake (CPE, e.g. with a return period equal to 975 years corresponding to a probability of exceedance of 5% in 50 years [18]), should also be controlled. To this end: 1) a ductile behavior of the retrofitted system should be guaranteed, and 2) the shear action on the floor diaphragms ($V_{floor,max}$) and on the foundation-system ($q_{foundation,max}$) should be controlled. To ensure the onset of a ductile behavior for CPE, the displacement to which the dissipative device is triggered d_{NL} (or the inter-story drift θ_{NL}) could be set to be less than the displacement demand for CPE (d_{CPE}).

Operative choices for LCT

An LCT based design aimed at minimizing environmental impacts along the building life cycle should also consider the adoption of sustainable operative choices such as eco-efficient materials, easily reparable and adaptable techniques, as well as components which are recyclable and reusable at the end of life. Moreover, as far as the social-economic sustainability of the seismic retrofit interventions is concerned, some operative choices could be undertaken to reduce the total costs of the intervention and minimize disruption of occupancy, potentially increasing the building renovation rate. With this aim, holistic solutions may be adopted to reduce the total cost of the intervention and the retrofit may be applied from the outside of the building to avoid the relocation of occupants. Interventions from outside poses instead additional challenges as to avoid construction works inside the buildings, which may require the adoption of innovative techniques, e.g. for the retrofit of existing diaphragms. It is worth noting that all the targets and the operative choices for the design of the retrofit intervention depend on the features of the existing building and on the selected retrofit intervention.

Finally, in order to control the behavior of the retrofitted building for the CPE, additional design choices may be required. For example, the damage occurring for such events may be lumped into few localized elements as to ensure the resilience of the retrofitted building. In the REDi protocol [17], ARUP proposed such an approach for the design of new buildings; however, this practice is not yet considered in the current design codes.

Table 1 Performance objectives (PO) for earthquake hazard level, design targets and further operative choices

	PO	Design targets	Design target motivation	Further operative choices
Environmental-economic sustainability *reduce impacts on the environment along the whole life cycle*	Operational performance for the *LSE*	$d_{LSE}<d_{TOP}$	*avoid damage on displacement, drift and acceleration sensitive elements to avoid repair costs and impacts, and building downtime for LSE*	*use of eco-efficient materials and techniques, easily reparable components, adaptable structural systems, and possibly recyclable and reusable components at the end of life (dry, prefabricated, standardized solutions)*
		$\theta_{LSE}<\theta_{MAX}$		
		$a_{LSE}<a_{floor,max}$		
Life safety and structural feasibility *a) guarantee the structural feasibility*	-	$q_{foundation,CPE} < q_{foundation,max}$ $V_{floor,CPE}<V_{floor,max}$	*no overloading of existing foundation (e.g. isolated footings not designed for seismic loads) and of floors for CPE*	-
b) guarantee the life safety and avoid injuries for LSE	Operational performance for the *LSE*	$V_{staircase,LSE} < V_{staircase,max}$	*ensure the operability of the egress path and avoid damage in NSE (responsible of injuries) for LSE*	-
		$\theta_{LSE}<\theta_{MAX}$		
c) guarantee a ductile behavior for CPE	Life safety performance and ductile behavior for the *CPE*	$d_{NL}<d_{CPE}$ *or* $\theta_{NL}<\theta_{CPE}$	*activate the dissipative devices before the CPE displacement (or drift) demand to ensure the onset of a ductile behavior for CPE*	*adoption of dissipative components localizing the damage and guaranteeing a ductile behavior for CPE, reducing post-earthquake repair works and building downtime.*
Social - economic sustainability *guarantee the economic and social feasibility of the intervention*	-	$\theta_{LSE}<\theta_{MAX}$	*avoid the relocation of the inhabitants with a retrofit assembled from the outside of the building (e.g. avoid damage in the infill walls, and avoid need for strengthening of the floors and staircase walls for LSE)*	*adopt holistic solutions to exploit synergies of the integrated interventions (i.e. sheared construction site, possible reinvestment of the tangible benefits of the energy retrofit to pay for the intangible benefits of the structural renovation etc.) reducing the LC total cost. Verify possible implementation of IHR plans.*
		$V_{floor,LSE}<V_{floor,max}$		

2.2 Structural design of diagrid exoskeletons

Diagrid systems are usually applied for the construction of new tall buildings. Accurate design procedures to determine the structural performances of these complex systems were investigated by different researchers [3, 10, 19, 14, 11, 13, 12]. When diagrids are proposed as strengthening solutions for RC buildings, the approach is revisited and adapted to the structural design of seismic-resistant exoskeletons.

2.2.1 Architectural and formal constraint

The structural performances of diagrids are strongly dependent on the geometry and the characteristics of their modules [20] (*Figure 2a*). The optimal module is a trade-off between architectural/formal needs and the envisioned structural performances. As for the diagrid architectural layout, it varies as a function of the building features. As far as the existing buildings are concerned, the additional diagrid exoskeleton has thus to comply with architectural and aesthetic needs (location of openings, inter-story height, vertical and planar irregularities, etc.). In addition, the new exoskeleton may be exploited as to enable possible expansions of the building's living space by introducing external rigid floor diaphragms (as, for instance, constituted by horizontal steel truss-works) that connect the existing building and the diagrid structure (*Figure 2b*). The detailing of such diaphragms goes beyond the scope of this paper and is a topic of ongoing research.

As far as the structural performances are concerned, Moon et al. [3, 10] showed that the optimal layout of the diagrid is a function of the diagonal element inclination. It was demonstrated that high inclination angles are optimal as to ensure maximum flexural stiffness compatibly with the geometric and technological limits of the diagrid modules, while an angle of 35° provides the maximum shear stiffness. It is thus expected that the optimal angle of the diagonal elements of a diagrid structure will range between these two values, and it will depend on the height and shape of the building.

Taking all these aspects into account, in this first step of the design, the inclination angle of the diagonals (Ψ) and the number of modules in the two principal directions (n_X and n_Y) should be defined.

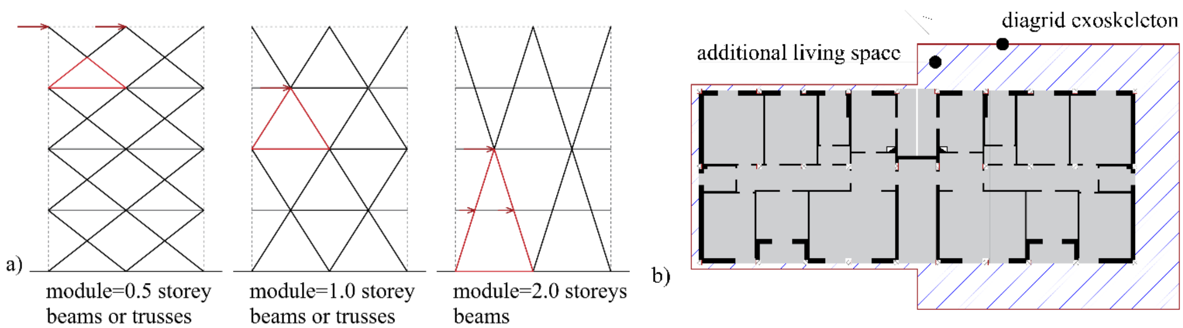

Figure 2 a) possible in-elevation configurations of the diagrid by varying the module geometry; b) possible in-plane configurations of the retrofitted structure in case of diagrid in adhesion or as an enlargement of the existing building.

2.2.2 Structural proportioning of the diagrid exoskeleton: diagonal's properties

Two alternative methods are proposed for the design of diagrid exoskeletons as innovative retrofit solutions. Both methods are based on the following assumptions: 1) the diagrid is elastic and over-resistant, and the connections are stiff; 2) the mass of the diagrid is negligible with respect to the mass of the existing building; 3) the elements of the diagrid have the same geometry (i.e. profile diameter and thickness at each floor along the same façade).

- *Method 1: combination of stiffness-based and strength-based design*

In this method the design of the diagrid elements is divided into 2 sub-steps: a) a stiffness-based design step, defining the minimum stiffness of the diagrid to control damage in the existing building, and the corresponding cross-section area of the elements ($A_d^{stiffness}$); b) a strength-based design step, determining the minimum cross-section area ($A_d^{strength}$) required to avoid buckling of the elements. The final cross-section area of the diagrid components is established as the maximum between the ones determined in the two design steps.

<u>*Stiffness-based design*</u>

In the case of seismic upgrade, the objective of the stiffness-based design is to control and limit the maximum displacement of the existing building when subjected to the design earthquake (e.g. LSE). This is aimed at minimizing the structural and non-structural damage in the case of a seismic event, thereby reducing the long-term disruption of the building activities, the relocation of occupants, and the costs for debris disposal and reconstruction. To this end, a target limit top displacement (d_{TOP}) aimed at reducing the damage to the existing building is selected and enforced for LSE, and the cross-section area of the diagrid diagonal elements that satisfies the displacement target is derived. As an example, for post-WWII European buildings, the target limit top displacement can be derived from the limit inter-story drift (θ_{MAX}) allowed by the infill panels considering that, in old RC buildings with sub-standard details, damage of non-structural components may occur before the onset of structural damage and it is responsible for a large part of building losses [21].

To evaluate the top displacement of the diagrid exoskeleton subjected to seismic loads, recent studies for the structural design of tall buildings are addressed [19, 14, 11], which demonstrated that the bearing system could be modeled as a cantilever deep beam, also taking into account the discrete nature of the diagrid. In such a structure, the shear deformation becomes significant, and the Timoshenko theory must be addressed. The procedure introduced by Baker [19] and analyzed by Mele et al. [11] for tall diagrids subjected to wind actions is here adapted for the retrofit of RC structures subjected to earthquakes, considering new load distribution applied to the simplified scheme. Nodal point loads distributed according to linear and mass-proportional modal shapes [18] are applied to the Timoshenko beam (*Figure 3a*, *b)* rather than the uniform load distribution modelling wind actions. Furthermore, in the case of stiff over-resistant diagrid exoskeletons and for regular and first-mode dominated RC buildings a triangular-distributed load *p* could be introduced to considerably simplify the analytical procedure and to generalize the equation of the Timoshenko beam (*Figure 3c,* [22]). In the case of existing RC buildings with average stiffness and geometries, this simplified load configuration does not introduce significant errors in the diagrid design for 4-storey or taller buildings: the top displacement is underestimated by at most 15% that obtained from the other two distributions [22]. On the other hand, in the case of low-rise buildings having less than 3 stories or for mass-proportional mode dominated RC buildings, the nodal point load configurations should be preferred.

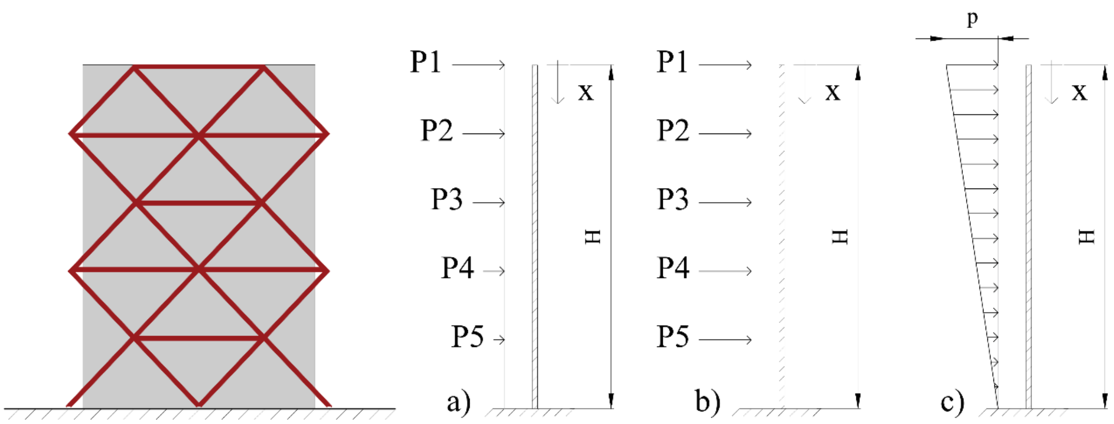

Figure 3 Different configurations of the loads on the Timoshenko beam for the simplified representation of the retrofitted system (existing building-diagrid): a) nodal point loads proportional to the first mode shape; b) nodal point loads with mass proportional distribution suitable for low-rise buildings; c) analytic simplification of the case a) with a triangular distributed load suitable in the case of 4-storey or higher buildings.

Solving the equations of a Timoshenko beam subject to a distributed triangular load (*Figure 3c*), the top displacement *y(0)* can be expressed as:

$$y(0) = \frac{1}{3}\frac{pH^2}{kA_sG} + \frac{11}{120}\frac{pH^4}{EI} \qquad \textit{Equation 1}$$

where E is the elastic modulus, k is the Timoshenko shear coefficient, and H is the building height. I and A_s are the area moment of inertia and the cross-section area of the diagonal elements. To account for the discrete nature of the diagrid system, the cross-section area and the moment of inertia of the Timoshenko beam are evaluated as follow [14]:

$$\begin{cases} A_s = 2n_w A_{d,W} \cos(\psi) \\ I = n_f A_{d,f} \sin(\psi) l^2 \end{cases} \qquad \textit{Equation 2}$$

where, n_w is the number of diagonals on the "web" façade (defined as the façade parallel to the horizontal action); n_f is the number of diagonals on the "flange" façade (defined as that orthogonal to the horizontal action direction); $A_{d,f}$ and $A_{d,w}$ are the cross-section area of the diagonal elements on the flange and web facades, respectively; l is the base length of the building in the direction parallel to the considered horizontal loads (*Figure 4*).

Once the load distribution, the diagrid layout, and the material properties are defined, the minimum cross-section areas that satisfy the stiffness constraint can be obtained ($A_d^{stiffness}$) by enforcing the maximum displacement $y(0)$ to be equal to the limit top displacement (d_{TOP}), and by considering the assumption that the same elements are adopted in each façade of the diagrid ($A_{d,w}=A_{d,f}$).

Strength-based design

In the diagrid design, buckling of the compressed diagonal members must be avoided. A simple procedure to estimate the axial forces in the diagrid components was proposed by Moon et al. [3], Mele et al. [12] and Montuori et al. [13, 14]. In the case of over-resistant elastic diagrid featuring one-floor-span modules (i.e. the height of the module is equal to the inter-story height) and made of truss elements, vertical and horizontal loads can be analyzed separately. In this model, gravity loads (P) are modelled as vertical point loads applied at each diagrid node, while seismic actions can be evaluated based on the assumption that the bending moment (M) is resisted by the diagrid "flange" façades, whilst the shear force (V) is counteracted by the diagrid "web" façades (*Figure 4*).

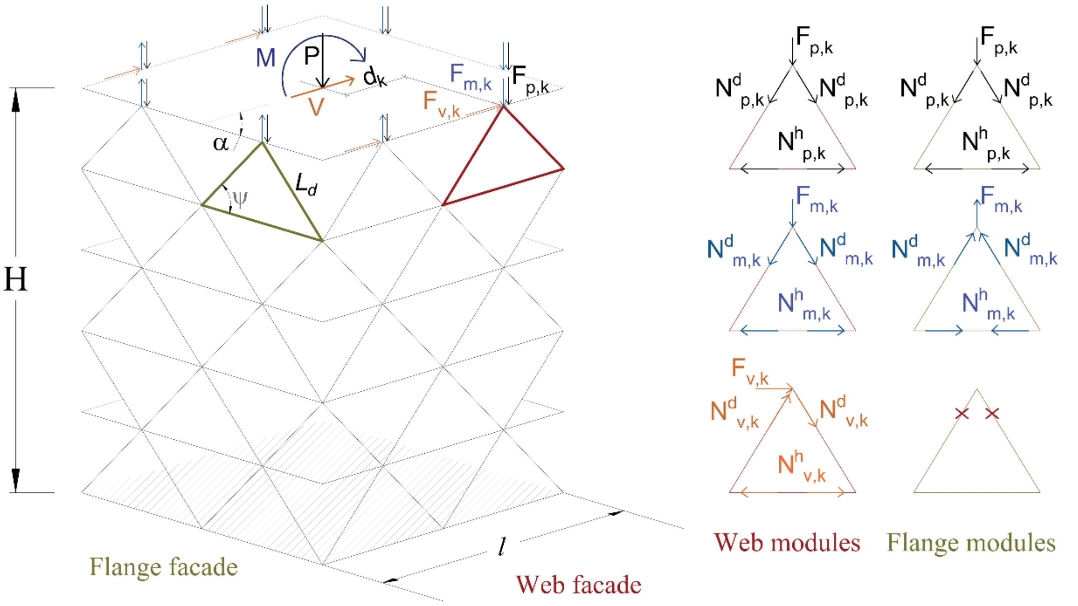

Figure 4 Internal actions in the diagrid structure due to gravity and lateral loads (after *[13]*), in which $F_{p,k}$, $F_{m,k}$ and $F_{v,k}$ are the forces in the k-th module due to vertical loads, overturning moment and shear force, respectively; $N_{p,k}$, $N_{m,k}$ and $N_{v,k}$ are the internal actions.

When the diagrid is subject to gravity and lateral loads, the axial force in the diagonal elements of the *k-th* module at the *j-th* floor can be calculated as follows [12]:

$$N_k = N_{p,k} + N_{m,k} + N_{v,k} = \frac{F_{p,k}}{2\cdot\sin(\psi)} \pm \frac{F_{m,k}}{2\cdot\sin(\psi)} \pm \frac{F_{v,k}}{2\cdot\cos(\psi)} = \\ = \frac{F_{p,k}}{2\cdot\sin(\psi)} \pm \frac{M_k d_k}{\sum_{i=1}^{n_k} d_i^2}\cdot\frac{1}{2\cdot\sin(\psi)} \pm \frac{V_k\cos(\alpha)_k}{\sum_{i=1}^{n_k}\cos(\alpha)_i}\cdot\frac{1}{2\cdot\cos(\psi)} \qquad \textit{Equation 3}$$

where $N_{p,k}$, $N_{m,k}$ and $N_{v,k}$ are the internal actions induced by the nodal forces in the *k-th* module due to vertical loads *(*$F_{p,k}$*)*, overturning moment *(*$F_{m,k}$*)* and shear force *(*$F_{v,k}$*)* respectively (*Figure 4*); d_k is the distance of the *k-th* module from the whole diagrid centroid axis, n_k is the number of the modules in the whole diagrid, and α is the angle between the lateral load direction and the web façade.

It is worth noting that Equation 3 only applies to one-floor-span modules. In the case of diagrids featuring higher modules extending over several floors, the elements' internal actions change quite remarkably as not only axial forces but also bending moments arise in the members [12].

To avoid buckling, the maximum axial compression action N_k of each structural member must be smaller than its design capacity N_k^{LIM} [18]:

$$N_k \leq N_k^{LIM} = \chi \frac{A_d \cdot f_{yk}}{\gamma_{M0}} \qquad \textit{Equation 4}$$

where A_d is the cross-section area of the diagonal element, f_{yk} is the characteristic yield strength, γ_{M0} is the material safety factor, and the coefficient χ is a reduction factor accounting for buckling. When considering the same cross-section area for each element of the diagrid, by substituting the maximum axial compression load in Equation 4, the minimum area of the diagrid elements according to the strength constraint ($A_d^{strength}$) can be derived through an iterative procedure. The choice of the boundary condition of the diagrid modules and, consequently, the effective length of the diagonals plays a critical role in this step of the design procedure.

- *Method 2: simplified design spectra combined with strength-based design*

The first considerations on the design of bracing systems through inelastic response spectra were made by Ciampi et al. [15] and were further developed in Feroldi [23], in which non-linear analyses on simplified FEM models were conducted for the design of retrofit solutions carried out from the outside. Stemming from these studies, an alternative method for the initial proportioning of the diagrid through the adoption of design spectra was defined [22].

Given the geometrical and mechanical properties of the existing building, the design spectra provide the minimum elastic stiffness that satisfies the target maximum displacement for the retrofitted building without solving the equation of the Timoshenko beam. These useful tools may thus simplify the preliminary design of retrofit interventions. The elastic stiffness of the diagrid affects the fundamental period of the retrofitted structure and, in turn, the maximum seismic action on the diagrid. Once the loads are known, the cross-section area of the diagrid members may be calculated by applying the strength-based design step previously introduced.

The definition of the design spectra is based on the assumption that, being the stiffness of the retrofitting diagrid exoskeleton (k_2) significantly higher than the stiffness of the existing building (k_1) and being the mass ratio between the existing building and the exoskeleton (m_2/m_1) lower than 1/10, the final system composed by the existing building and the diagrid can be modelled as a simplified single degree of freedom (SDOF) system [22] (*Figure 5*). The existing building is represented as an elastoplastic system with elastic fundamental period T_1, mass m_1, initial elastic stiffness k_1 and damping coefficient c_1, whose backbone curve is defined by the yielding force F_{y1}, yielding displacement δ_{y1} and ultimate displacement δ_{u1}. The diagrid, which is designed to be elastic and over-resistant, is represented by its stiffness k_2 and the damping coefficient c_2. Finally, the connection system, assumed as elastic, is defined by the stiffness k_{12} and the damping coefficient c_{12} (*Figure 5*).

By modelling the connection and the diagrid as two springs in series k_{12} and k_2, the equivalent stiffness of the retrofit can be expressed as:

$$\tilde{k} = \frac{k_2 k_{12}}{k_2 + k_{12}} \qquad \textit{Equation 5}$$

In the hypothesis of rigid links connecting the existing building and the diagrid, it can be assumed that the equivalent stiffness $\tilde{k}$ is equal to the stiffness of the diagrid k_2 ($\lim_{k_{12}\to\infty} \tilde{k} = k_2$). Similar considerations may be made for the damping coefficient $\tilde{c}$. The assumption of elastic and rigid connections could be reasonable considering that, by exploiting the extension of the diagrid façades, the connections between the existing building and the diagrid can be distributed along the entire perimeter beams, allowing for the adoption of a large number of connectors and for the reduction of the transferred loads.

The final system may thus be described as a SDOF system characterized by a backbone curve with initial stiffness $\hat{k}$ equal to the sum of k_1 and $\tilde{k}$ up to the yielding displacement δ_{y1} and a stiffness equal to $\tilde{k}$ up to the ultimate displacement δ_u.

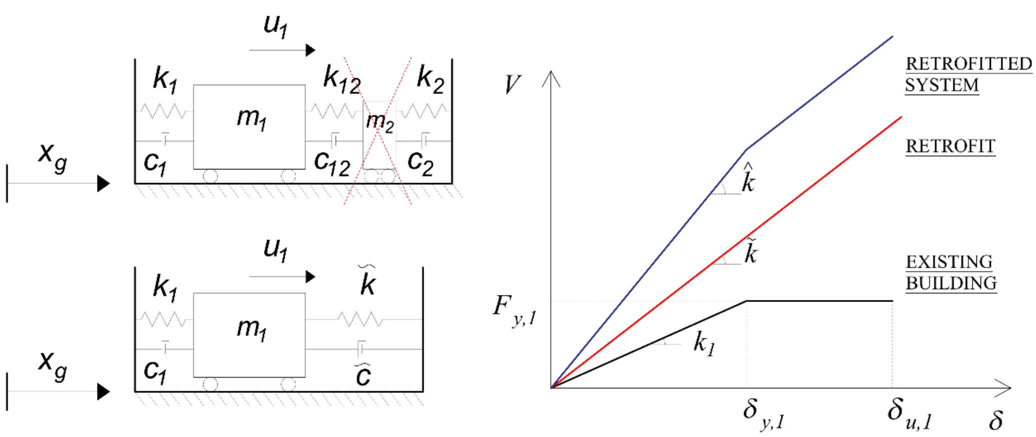

Figure 5 SDOF model. Simplified SDOF system (left); response curve of the 2 degrees of freedom (right).

Following the nomenclature introduced by Ciampi et al. [15] and Feroldi [23], some adimensional parameters are introduced to simplify and generalize the spectra:

- the "strength parameter" η represents an estimation of the strength of the existing building against the seismic action, and is defined as the ratio between the RC building yielding force $F_{y,1}$ and the associated elastic seismic demand ($m_1 \cdot S_a(T_1)$):

$$\eta = \frac{F_{y,1}}{[m_1 \cdot Sa(T_1)]} \qquad \textit{Equation 6}$$

- the "ductility demand" of the existing building μ represents the damage on the existing building after the retrofit and is defined as the ratio between the maximum displacement δ_{MAX} experienced by the RC building after the retrofit and the yielding displacement $\delta_{y,1}$:

$$\mu = \frac{\delta_{MAX}}{\delta_{y,1}} \qquad \textit{Equation 7}$$

- the "stiffness ratio" $\tilde{\lambda}$ is defined as the ratio between the equivalent elastic stiffness of the retrofit $\tilde{k}$ (Eq.5) and the initial elastic stiffness of the existing building k_1:

$$\tilde{\lambda} = \frac{\tilde{k}}{k_1} \qquad \textit{Equation 8}$$

Design spectra are defined by carrying out sensitivity analyses for varying the properties of the simplified SDOF system, and they plot the ductility demand of the existing building (μ) as a function of the stiffness ratio ($\tilde{\lambda}$) with the purpose to evaluate how the elastic stiffness of the retrofit ($\tilde{k}$) affects the response of the SDOF system in terms of maximum deformability (δ_{MAX}).

Once the target displacement is defined, the elastic period ($\overline{T}$), the spectral acceleration ($S_a(\overline{T})$) may be derived from the response spectra; consequently, the total stiffness ($\hat{k}$) and the seismic action $\hat{V}$ on the final system (building+diagrid) may be calculated. According to the initial stiffness of the building (k_1) and its maximum capacity ($F_{y,1}$), the stiffness of the diagrid $k_2 = \tilde{k}$ and its seismic load (V_2) are then calculated. A layout of the procedure adopted to derive the design spectra is represented in *Figure 6*; details on the construction of the design spectra may be found in Labò et al. [24].

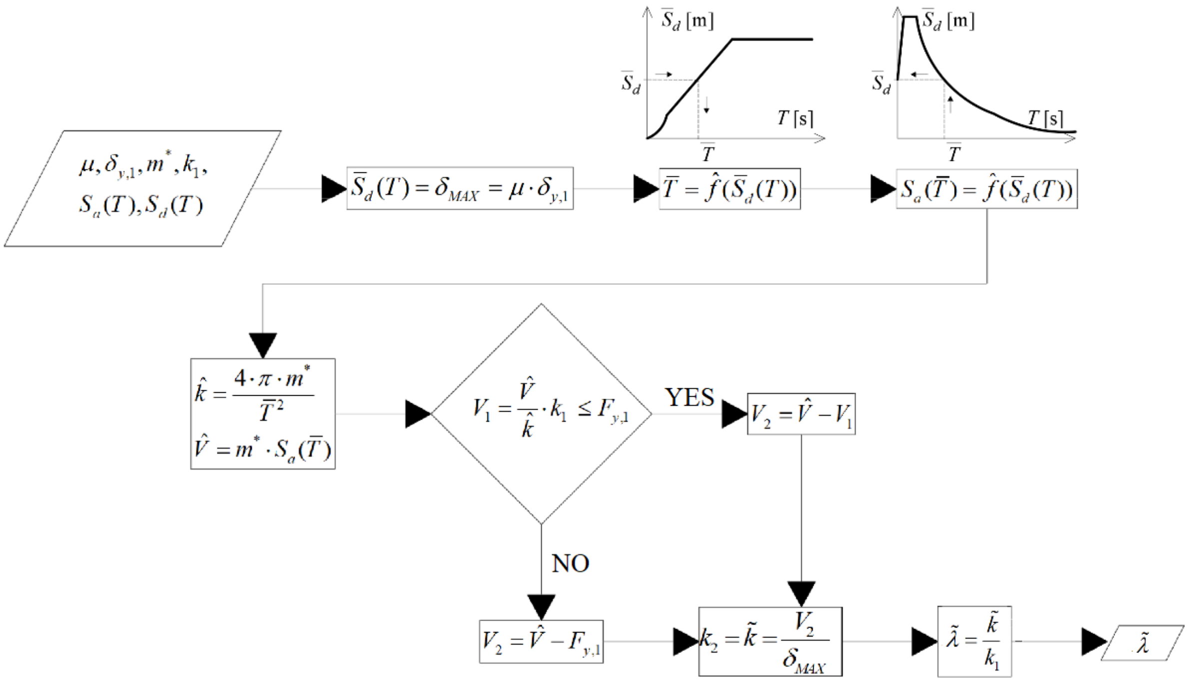

Figure 6 Layout of the procedure to determine the parameters used in the definition of the design spectra (after *[24]*). The simplified procedure is based on the assumption that the mass matrix of the retrofitted building can be assumed as equal to the mass matrix of the existing building (m^*). Starting from the ductility factor μ all the parameters used to correlate μ and the stiffness ratio ($\tilde{\lambda}$) of the design spectra can be derived as shown in Figure.

Figure 7 introduces the design spectra for the preliminary proportioning of the diagrid exoskeleton for a given value of the initial period (T_1) of the building in the AS-IS situation and for different values of the strength parameter (η). It should be noted that since the results of the sensitivity analysis are expressed in terms of the strength parameter (η), the results are normalized with respect to the elastic demand and, therefore, they can be applied in areas with different seismicity. In Appendix A, five design spectra for the preliminary design of diagrid exoskeletons are reported considering different values of T_1 (*Table 2*). The spectra are obtained by varying the input parameters of the SDOF system as reported in *Table 2*. The input parameters are selected to be representative of the typical post-WWII RC buildings, generally made of reinforced concrete frames with masonry infill walls, according to [[25], among others]. Simplified systems with elastic period ranging from 0.6 s to 2.5 s and different masses are considered to represent RC infilled frames featuring different height (2 through 10 floors), in-plan dimension and bearing systems. As for the yielding force, different values of η were considered to represent weak (η=0.30), medium (η=0.50-0.60) and strong (η=0.85) buildings as proposed in [23].

Table 2 Inputs used in the sensitivity analysis of the elastic SDOF system.

Parameter	**Symbol**	**Range**
Elastic period	T_1	0.5-2.5 [s]
Effective mass	m_1	451-800-1000 [kN/g]
Elastic stiffness	k_1	7.5-13-24 [kN/mm]
Strength parameter	η	0.30-0.50-0.60-0.85 [-]

The solutions $\tilde{k}$ are plotted in the range $(0\div6)k_1$, in which $\tilde{k}$=0 represents the AS-IS condition and $\tilde{k}=6k_1$ is considered a reasonable limit for equivalent retrofit stiffness [23].

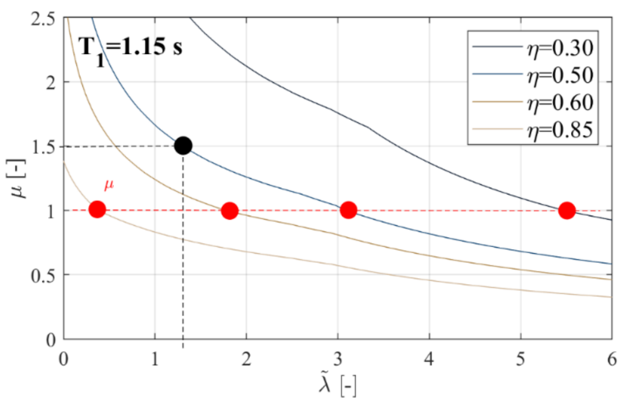

Figure 7 Evaluation of the ductility demand (μ) as a function of the retrofit stiffness ratio ($\tilde{\lambda}$) for varying adimensionalized yielding force of the existing building (η). "R" refers to the reference case presented in section 4. The red dashed line represents a unitary value of the ductility demand (μ).

As expected, the response of the SDOF system depends on the elastic stiffness of the retrofit solution (*Figure 7*). Maximum damage on the building, corresponding to the maximum values of the ductility demand parameter μ, corresponds to the AS-IS condition (or no-retrofit condition, $\tilde{\lambda}$=0). For a fixed value of T_1, the ductility demand decreases as the stiffness ratio increases, i.e. the stiffer is the diagrid the lower is the damage on the existing building. For a given stiffness ratio $\tilde{\lambda}$, the ductility demand increases for decreasing values of η, i.e the weaker is the existing building the higher is the damage; whilst for a given μ (so for a given target maximum displacement), the required $\tilde{\lambda}$ increases for decreasing values of η, i.e. the lower the strength of the existing building the higher the stiffness of the retrofit ($\tilde{k}$) must be.

Finally, an upper bound to the value of λ can be set to ensure the technical feasibility of the retrofit solution. Looking at *Figure 7*, for high values of λ, it is not beneficial to further increase the stiffness of the retrofit since it would only lead to a slight reduction of the ductility demand μ. This assumption may lead to the definition of an upper bound on the values of the retrofit stiffness.

2.3 Diagrid design procedure

A new procedure to design a diagrid exoskeleton for the seismic retrofit of an existing RC building is thus proposed, which may be summarized in the following steps:

Step 1) Definition of the SDOF system equivalent to the existing building (Γ, T_1, m_1, k_1, F_{y1}, δ_{y1}, δ_{u1})

Step 2) Definition of performance objectives and design targets respectful of LCT principles, intention to work from outside, and taking into account the main features of the RC buildings. Possible performance objectives may encompass, for instance, the need to protect existing floors with limited in plane capacity, the need to protect stiff staircase cores not designed to withstand horizontal loads and the need to control damage in infill walls, among others. The corresponding design targets may be expressed in terms of: d_{TOP}, θ_{max}, $V_{floor,max}$, $V_{staircase,max}$, $q_{foundation,max}$.

Step 3) Definition of the geometry of the diagrid according to aesthetic and formal constraints (Ψ, n_X, n_Y)

Step 4) Design of the minimum cross-section area of the diagrid diagonal members ($A_{d,w} = A_{d,f} = A_d$)

- Method 1 – stiffness-based and strength-based design ($A_d^{stiffness}$; N_k, $A_d^{strength}$; A_d = max ($A_d^{stiffness}$, $A_d^{strength}$))
- Method 2 – design spectra (η, μ; $\tilde{\lambda}$; k_2; N_k; A_d) and strength-based design

Step 5) Validation through nonlinear numerical analyses modelling the whole structure

2.4 Considerations about the behavior of the retrofitted building at collapse

For the definition of the behavior of the diagrid beyond the life safety limit state, 2 solutions are generally possible: an elastic solution and a non-linear solution. In the latter, for instance, dissipative links could be included in the diagonals of the diagrid at the ground floor. The first solution leads to an elastic behavior of the diagrid even at the collapse prevention limit state. However, in such a case, the load conditions in the diaphragms and in the foundations may be critical. At this regard, it is advisable to limit the system demand beyond the life safety limit state to avoid overloads in the system components and at the foundation level. This could be accomplished by the second solution, where, through a non-linear behavior of the diagonals at the ground floor, the behavior of the retrofitted building would be more controlled and ductile. It is worth noting that in such conditions an increase of demand to structural and non-structural elements at the ground floor is observed: indeed, such elements are subject to greater inter-story displacements compared to the elastic solution, and local interventions could be envisaged to increase the ductility of the structural elements and to limit the interaction with the infills.

The activation load of the dissipative links (for example by means of hysteretic or friction-based systems) in the diagonals at the ground floor may be evaluated as the load corresponding to LSLS. In this way it is possible to: 1) set an upper limit to the soliciting actions that allows the control and limitation of the actions in the diaphragms and in the foundation system; 2) ensure a ductile behavior of the retrofitted building at CPLS; 3) localize damage and deformations in some dissipative links to reduce repair works in the case of an exceptional event.

3. Application to a reference building

In order to highlight the effectiveness of the diagrid exoskeleton in the retrofit of vulnerable existing RC buildings, a reference building was analyzed. In the initial proportioning of the diagrid, the design procedure illustrated in Section 2 was applied. The reference structure is a RC building located in Brescia (Italy), which presents common features of typical 70s-80s European buildings (*Figure 8*).

Figure 8 Views of the reference building *[26]*.

The structure was built in 1975 according to the regulation codes and the construction techniques of the time. Main features and structural details of the reference building were derived from the original construction documents, from the technical report of a diagnostic campaign [26], and by direct visual inspection [27, 22].

The reference structure is an 8-story rectangular building (27.10 m x9.35 m) featuring three one-way longitudinal frames (F1-F3) and two infilled lateral frames (F4, F5). The inter-story height (h_i) is equal to 2.50 m at the ground floor and 3.20 m at the upper floors, for a total height of 24.80 m. The bearing structure is made of RC frames and was designed for vertical loads only; the frame spans range between 2.5 m and 3.6 m in the longitudinal direction, whereas between 4.25 m and 5.10 m in the transversal direction (*Figure 9*).

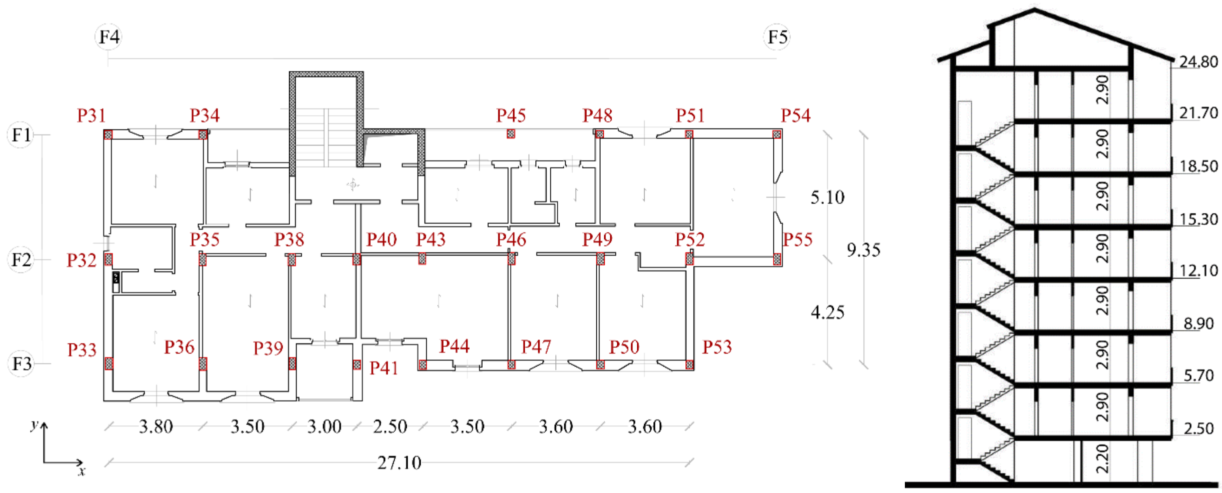

a) b)

Figure 9 Plan of a reference floor (left); Transversal section of the reference building (right).

The characteristics of the steel rebars in the frame elements were investigated through magneto-metric tests [26], and the results for each element are reported in Appendix B. Floors are made of a one-way RC beams and clay blocks floor system featuring a 2.5 cm RC overlay for a total thickness of 24 cm. The staircase core is a RC C-shaped shell; however, since the structural detailing was not conceived to ensure a global behavior among the three walls, they are regarded as three independent walls. The thickness of the stairwell walls varies between 20 cm and 25 cm. The structure lays on direct pile foundations and on additional RC walls introduced during a retrofit intervention on the foundation system carried out in the 1983.

As for the non-structural elements, infill panels are made of one-layer hollow bricks with two outer layers of plaster [26].

The material properties of the RC frame were derived from the results of the compressive tests on concrete and tensile tests of the steel rebars [26]. Accordingly, concrete C25/30 and steel Feb44k (design yielding stress equal to 430 MPa) are considered.

The preliminary analysis of the available construction documents and rapid visual inspection of the building highlight some inherent deficiencies that could detrimentally affect the structural response in the case of an earthquake, namely:

- vertical irregularities: at the ground floor, the absence of the infill panels may result in severe damage and stress concentration in the columns of this floor leading to the onset of a possible soft-story mechanism;
- in-plan irregularities: the in-plan asymmetric staircase core significantly affects the position of the shear center, thus introducing some torsional mode shapes that may increase the displacements and the stresses in localized parts of the structure.
- the building was not conceived to withstand seismic loading.

3.1 Numerical analysis of the structural response

The finite element model was developed with the software MidasGen (2018) [28]. The frame components were modeled as beam elements and their inelastic behavior was accounted for by means of lumped plastic hinges in which the flexural and the shear behavior of the frame elements were modeled with the degrading Takeda constitutive law [29]. More precisely, the flexural plastic hinge is a trilinear curve followed by a degrading branch (*Figure 10a*), while the shear plastic hinge has a linear behavior up to the ultimate capacity; beyond that limit, the curve decays abruptly with a sudden brittle failure (*Figure 10b*).

The ultimate shear resistance (V_{Max}; ξ_{Max}, *Figure 11b*), and the characteristic points of the flexural curve - cracking (M_{cr}; φ_{cr}), yielding (M_y; φ_y), ultimate (M_u; φ_u), and residual (M_{res}; φ_{res}) (*Figure 11a*) - were calculated based on the formulations suggested from European [18] building codes.

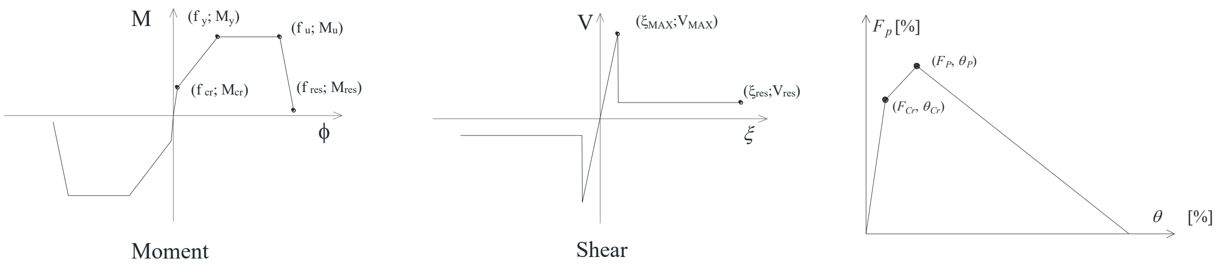

a) b) c)

Figure 10 a) Flexural behavior; b) shear behavior; c) axial behavior of the compression-only diagonal struts. In the axial plastic hinge, the forces are normalized by the peak value.

The building floors were assumed to withstand horizontal loads by developing an in-plane tied-arch (or strut and tie, [30]) resistant mechanism up to their ultimate capacity [31, 32]. The maximum actions in the diaphragm were assessed to be smaller than the maximum capacity of the existing floors.

The infill panels were modeled as two compression-only diagonal struts converging in the beam-column joints as recommended by [33] among others. The non-linear behavior of the infills is described by means of a trilinear axial plastic hinge defined by the cracking (F_{cr}; θ_{cr}) and the peak (F_P; θ_P) points (*Figure 10c*). The cracking force F_{cr} and the peak force F_P were evaluated according to Decanini et al. (1993), while the cracking drift θ_{cr} and the peak drift θ_P were set to in accordance to the common values of 0.3% drift for minor cracking and 0.5% drift for the infill failure [34] (*Figure 10c*).

Since the staircase walls were not designed to withstand the horizontal loads, the same considerations adopted to model the infill panels were considered for these elements, and they were modelled as rigid elements with low ductility.

The structural response of the existing building was evaluated by means of non-linear static analyses. The Pushover curve in the weakest direction of the building (y-direction in *Figure 9*) is reported in *Figure 11a,* in which some relevant points of the curve are highlighted. Infill cracking, at the ground level, occurs at 27 mm displacement, while infills failure, at the ground level, occurs at 78 mm; plastic hinges develop at the ground floor columns and the onset of soft story induces a plastic behavior up to 120 mm. Then an abrupt loss of resistance is observed due to (as expected) a soft-story mechanism at the ground floor that causes a brittle collapse of the existing building (*Figure 11c*). According to the current code, the Life Safety Limit State (LSLS) and the Collapse Prevention Limit State (CPLS) are indicated in the capacity curve (with full colored dots) [35]. The CPLS is considered in correspondence to the lateral displacement of the structure at the onset of the soft story mechanism. The LSLS limit is considered is achieved at ¾ of the ultimate rotational capacity of the columns at the ground floor [35].

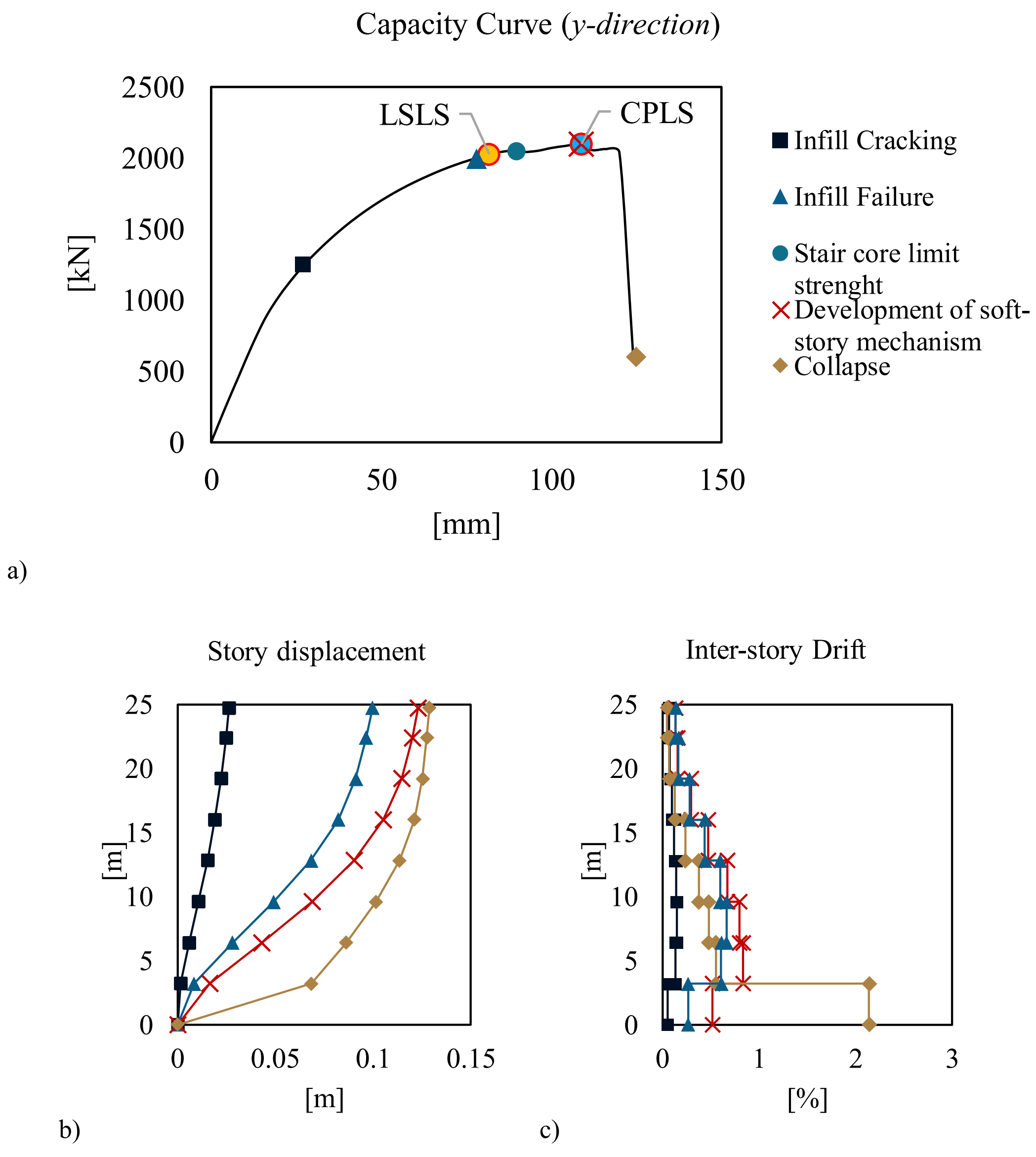

Figure 11 a) Capacity curve in the *y*-direction, b) story displacement and c) inter-story drift.

The vulnerability analysis of the existing building was then conducted, according to the N2 method [36], considering the building as located in Brescia (Italy), on a flat surface made of deposit of sand or medium-dense sand gravel or stiff grave (soil category C and T1 topography) [35] The main parameters of the N2 method, which define the properties of the equivalent SDOF system, are reported in *Table 3*.

Table 3 N2 method main parameters.

Parameter	**Symbol**	**Value**
Participation factor	Γ	1.40
Yielding force of the bi-linear curve	F_{y1}	1424 kN
Yielding displacement of the bilinear curve	δ_{y1}	0.031 m
Ultimate displacement of the bilinear curve	δ_u	0.07 m
Fundamental period of the equivalent SDOF system	T_1	1.15 s
Mass of the equivalent SDOF system	m_1	1568 kN/g
Stiffness of the equivalent SDOF system	k_1	45450 kN/m
Displacement Demand for the SDOF system for the Life Safety Earthquake (LSE)	S_d^{LSE}	0.07 m
Displacement Demand for the SDOF system for the Collapse Prevention Earthquake (CPE)	S_d^{CPE}	0.09 m

The bi-linearized capacity curve and the displacement demands (S_d^{LSE} and S_d^{CPE}) are plotted in the Acceleration Displacement Response Spectrums (ADRS) related to Life Safety Earthquake (LSE) and Collapse Prevention Earthquake (CPE) (*Figure 12*). In this case, being the period of the retrofitted building (T) higher than T_C (end of the constant acceleration region of the spectrum), the equal displacement rule is considered.

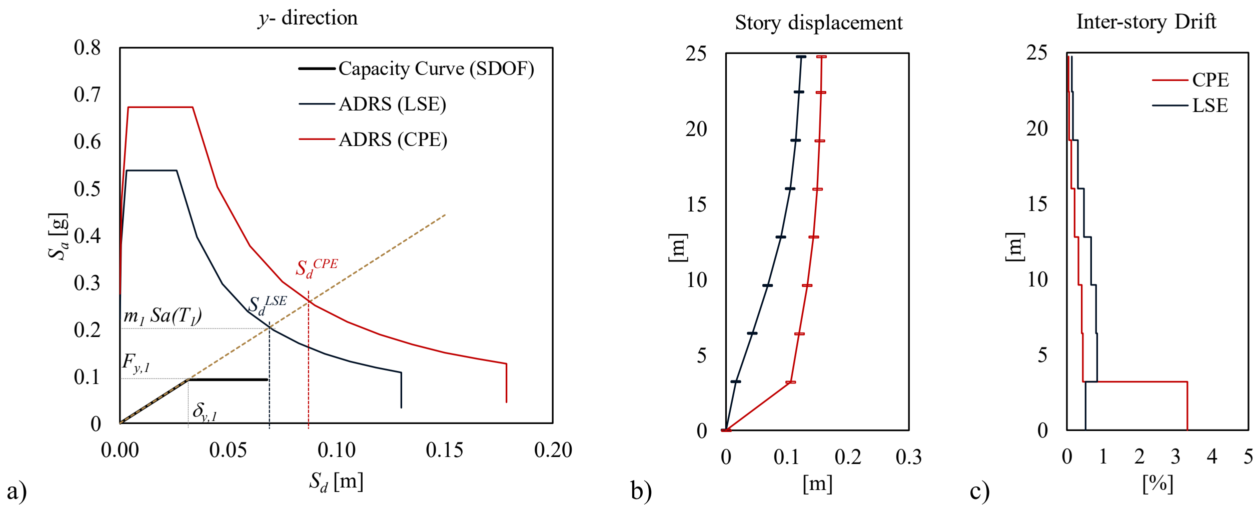

Figure 12 a) ADRS and displacement demands; b) Story displacement; c) inter-story drift (right) at the considered displacement demands.

To critically evaluate the results, some considerations are needed:

- the displacement demand related to the LSE lies in correspondence to the capacity curve failure point, meaning that a sudden failure of the existing building may occur for a seismic event slightly higher than that expected in the design spectra;
- the Finite Element Model is characterized by several uncertainties that may affect the response of the existing building. Uncertainties are related to unexhaustive knowledge of material properties and structural details (such as beam-column joint reinforcement), and other uncertainties are related to the numerical modeling, particularly with reference to the calibration of the plastic hinges of the infill panels and of the staircase core. Ignoring these main issues may result in the assembly of erroneous numerical models having structural responses remarkably different from the actual one [37];
- 1.0% inter-story drift related to the LSE (*Figure 12*) entails the failure of the infill panels and severe and extended damage on the existing building, resulting in high expected repair costs and building downtime;
- the stairwell, that represents the only egress path of the building, is severely damaged in case of LSE.

For these reasons and considering that the existing building does not satisfy the displacement demand related to the LSE and CPE (*Figure 12*), the structural retrofit is envisioned.

3.2 Design of the diagrid exoskeleton

The seismic retrofit of the building is obtained by introducing an elastic and over-resistant diagrid exoskeleton, whose preliminary design is carried by addressing the design procedure introduced in Section 2.

3.2.1 Step 1

In this example, since the vulnerability of the existing building was estimated by means of nonlinear static analyses, the properties of the equivalent SDOF system have already been calculated (*Table 3*).

3.2.2 Step 2

In order to achieve the retrofit performance objectives, specific design targets were defined. A maximum inter-story drift equal to 0.3%, avoiding non-structural element damage in case of LSE as recommended by [34], and a maximum base shear flow equal to 250 kN/m, guaranteeing feasibility of the new foundation system made of RC beams and micropiles [27], were considered. A maximum floor shear action of 650 kN was considered to avoid exceeding the ultimate floor in-plane capacity. The floor capacity was evaluated with reference to [23] considering the floor able to resist in-plane forces by developing an arch resistant mechanism spanning between two opposite diagrid facades, thus having the span corresponding to the length of the building[1].

3.2.3 Step 3 - Architectural aspects and internal actions

The diagrid was conceived to be in close proximity to the building in the y-direction and as an enlargement in the x-direction. This way, new living spaces can be added in the longitudinal direction, thereby increasing the potential economic value of the retrofitted building. Considering an optimal angle for shear building of 35° [10] and setting the diagrid module height h as equal to the inter-story height of the existing building h_i, an

---

[1] This resistance has been calculated as: $V_f = 2 \cdot \left(\frac{1}{2}\,\tau_{brick}\,H\,t_{eq}\right)$ where $\tau_{brick} = 1.74MPa$ is the ultimate shear resistance of the brick/joists system, which was determined in an experimental campaign [23], *l=9.35m* is the height of the floor and *t=40mm* is the height of the RC slab [31].

inclination angle of the diagonals ψ equal to 38.9° was adopted. The diagrid exoskeleton was assumed to be made of S355 steel pipes with the same cross section in the two main directions. The resulting diagrid layout and geometry are shown in *Figure 13* and *Table 4*. Due to the vertical irregularity of the existing building, the diagonal length L_d is equal to 3.98 m and 5.02 m at the ground floor and at the upper floors, respectively.

Table 4 Geometry of the additional diagrid exoskeleton.

Parameter	**Symbol**	**Value**
Existing building height	H	24.75 m
Diagonal angle	Ψ	38.9°
Number of diagonals in the web façade	n_w	4
Number of diagonals in the flange façade	n_f	8
Dimension of the web façade	L	15.90 m

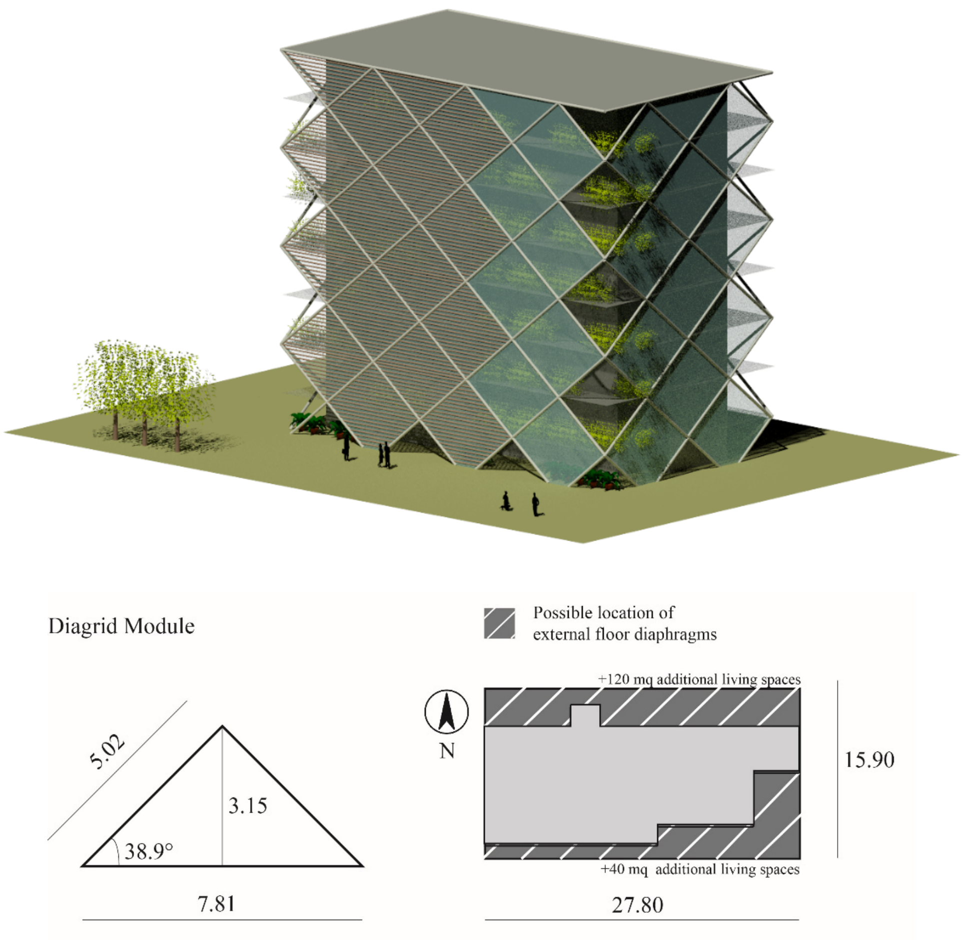

Figure 13 Architectural and formal aspects of the retrofit solution.

3.2.4 Step 4

The two alternative design methods discussed in Section 2 are applied for the design of the diagrid elements.

- *Method 1 – stiffness-based and strength-based design*

The external load of the Timoshenko beam and the shear and the bending moment at each floor of the diagrid were derived as a function of the total base shear of the retrofitted building (V), expressed as:

$$V = m_1 \cdot Sa(\bar{T}) \cdot \Gamma_{FIN} \qquad \textit{Equation 9}$$

where Γ_{FIN} is the participation factor of the retrofitted building (calculated considering the mass matrix of the existing building and a linear deformed shape of the retrofitted building), and $Sa(\bar{T})$ is the design spectrum acceleration derived as a function of the target spectrum displacement $\bar{S}_d(T)$. In particular, $\bar{S}_d(T)$ can be expressed as the ratio between the target displacement d_{TOP} and the participation factor Γ_{FIN}, where d_{TOP} is derived by multiplying the inter-story target (θ) by the existing building height (H).

The retrofitting diagrid was considered as a Timoshenko beam subjected to a triangular distributed load (p) equal to $2V_2/H$, where V_2 is the base shear of the diagrid (derived starting from the total base shear - V, Eq.9) and considering that the existing building and the diagrid behave like two elastic systems in parallel. By combining Equation 3 and Equation 1, and by enforcing $y(0)$ equal to the target displacement d_{TOP}, the cross-section area of the diagonal elements $A_{d,W} = A_{d,f}$ that satisfy the stiffness constraint was derived.

By imposing a tubular thickness ($s_{stiffness}$) of 10 mm, the element diameter ($\Phi_{stiffness}$) equal to 131.0 mm was obtained. The enforcement of the stiffness constraint leads to an equivalent stiffness of the retrofit equal to $\tilde{k} = k_2$=60.63 kN/mm (k_2=1.33k_1).

The strength-based design step is carried out to avoid the buckling of the diagonal elements; according to (Equation 3), the axial forces in each module of the diagrid were calculated by adopting a seismic force equal to V_2. It is worth noting that, if the diagonal cross-section obtained from the strength-based design leads to an equivalent stiffness of the retrofit significantly higher than the equivalent stiffness obtained from the stiffness-based method, the total base shear (V) should be redefined, and an iterative procedure should be considered.

In the reference case, the dead loads of the diagrid exoskeleton were neglected because their magnitude was negligible and would entail a ±1% axial force. The resulting forces are reported in *Figure 19*.

The profile characteristics ($\Phi_{strength}$, $s_{strength}$) were determined by combining the maximum axial force of the diagonals and the maximum capacity of the commercial profiles for given effective length L_0 of the diagonals. In *Figure 14*, to evaluate how the different parameters can affect the results, Equation 4 was plotted for fixed values of the yield strength f_{yk} and the maximum drift target θ for varying profile diameters ϕ; in *Figure 15*, different thicknesses of the elements were also considered.

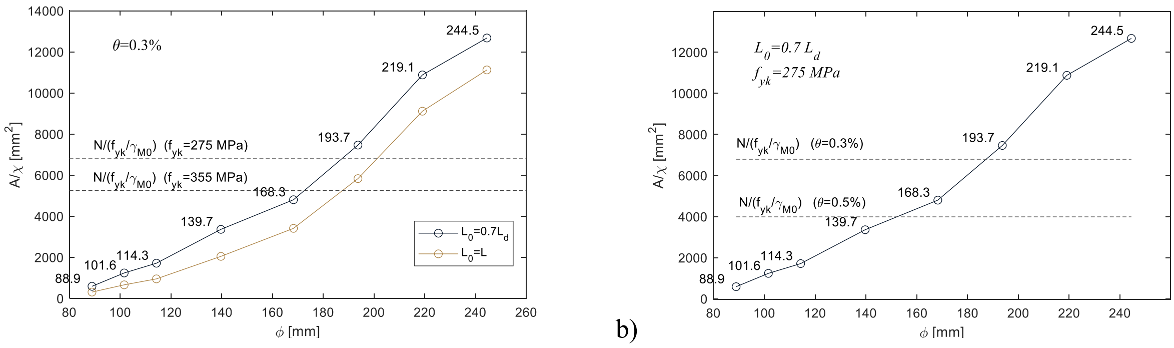

a) b)

Figure 14 Commercial profile capacity as a function of the technological aspects. a) by varying the boundary condition and the material properties; b) by changing the drift target.

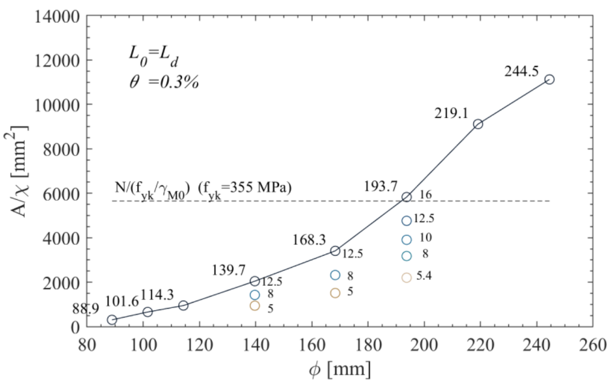

Figure 15 Comparison of the maximum axial force in the diagonals

and the maximum capacity of the commercial profiles for varying diameters and varying thicknesses of the profile.

In the reference case, considering the diagonal elements as pinned at each end, a diagrid structure made of S355 steel, and an inter-story drift ratio target equal to 0.3%, the required minimum profile has (*Figure 15*) diameter ($\Phi_{strength}$) equal to 193.7 mm and tubular thickness ($s_{strength}$) of 16 mm which leads to a diagrid exoskeleton stiffness equal to $\tilde{k}$ =k_2=173.9 kN/mm=3.9k_1.

The design profile diameter Φ_{FIN} was derived as the maximum between $\Phi_{stifness}$ and $\Phi_{strength}$.

$$\begin{cases} \Phi_{FIN} = 193.7\ [mm] \\ s_{FIN} = 16.0\ [mm] \end{cases}$$

It is worth noting that, in this case, buckling plays a fundamental role in determining the minimum cross-section area of the profile; for the reference building, the stiffness constraint becomes a priority when the inter-story drift target is set equal to or smaller than 0.2%. In the future, more accurate buckling analyses considering the joint stiffness are envisioned to define smaller profiles.

- *Method 2 – design spectra and strength-based design*

Similar results were obtained from the simplified design spectra procedure. The input parameters are the period of the equivalent SDOF system T_1=1.15 s, the ratio between the yielding force of the existing building (F_{y1}) and the associated elastic seismic demand (m_1*$Sa(T_1)$) η=0.50, which results from the ADRS, the target ductility demand μ=1.5, which is derived by enforcing the maximum displacement δ_{MAX} as equal to the target displacement of the existing building d_{TOP} divided by the participation factor Γ_{FIN}.

From the design spectrum reported in *Figure 7*, a stiffness of the diagrid intervention $\tilde{k}$=1.30k_1 is determined. Knowing the total stiffness ($\hat{k}$) and the mass (m^*) of the whole system, the elastic period ($\bar{T}$) of the retrofitted system can be derived from the displacement spectrum, and the associated seismic demand ($S_a(\bar{T})$) can be calculated. Consequently, the maximum forces in the elements and their cross-section area may be defined by applying the strength-based method.

3.2.5 Step 5

The pushover of the existing building after the retrofit (*brown*), and of the existing building in the AS-IS condition (dashed line) are reported in *Figure 16*a. As concern the retrofitted building, 2 solutions are reported: an elastic solution (*grey*) and a non-linear solution in which a non-linear behavior is introduced in the diagrid diagonal at the ground floor (*blue*). Both the solutions are elastic up to the Life Safety Earthquake (LSE), in order to meet the defined targets; specific considerations about the behavior of the retrofitted building beyond the LSE are made in the next section. Moreover, in *Figure16a*, the red crosses indicate the buckling of the diagonal elements at the base of the diagrid, the squares represent the infill cracking along the height of the existing building and the rhombus the failure of the new external diaphragm. Beyond failure, the diaphragm is no longer able to transfer the seismic loads from the existing building to the diagrid exoskeletons; for this reason, the capacity curve is dashed. Finally, when the diagonals buckle, the capacity curve is interrupted since a sudden decrease of the capacity due to the elasto-fragile behavior, introduced to represent the compressed diagonals, does not guarantee the control of response and damages of the retrofitted structures. This scenario does not fit with the selected performance objectives and, therefore, it is not accepted in the retrofitted buildings. *Figure 17a* shows that the displacement demand related to the CPE is satisfied and buckling in some diagonals occurs for larger displacements. The deformed shape of the retrofitted building at the LSE (*Figure 16*b) can be considered as linear, and the inter-story drift satisfies the imposed target limit (*Figure 16*c). Considering a linear deformed shape and a maximum inter-story drift target equal to 0.3%, the target displacement in Figure 16b can be obtained from multiplying θ_{MAX} by the building height.

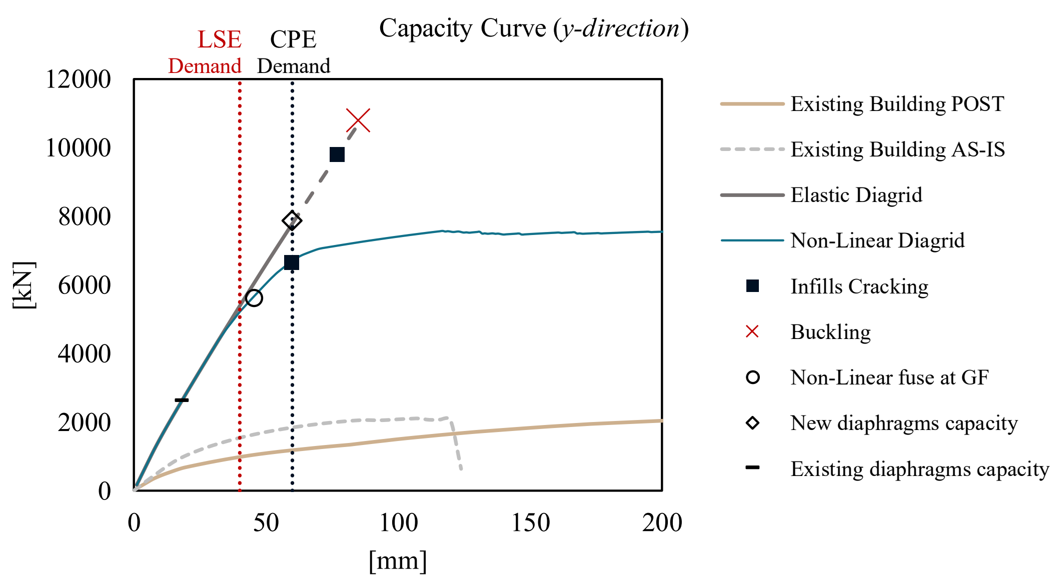

a)

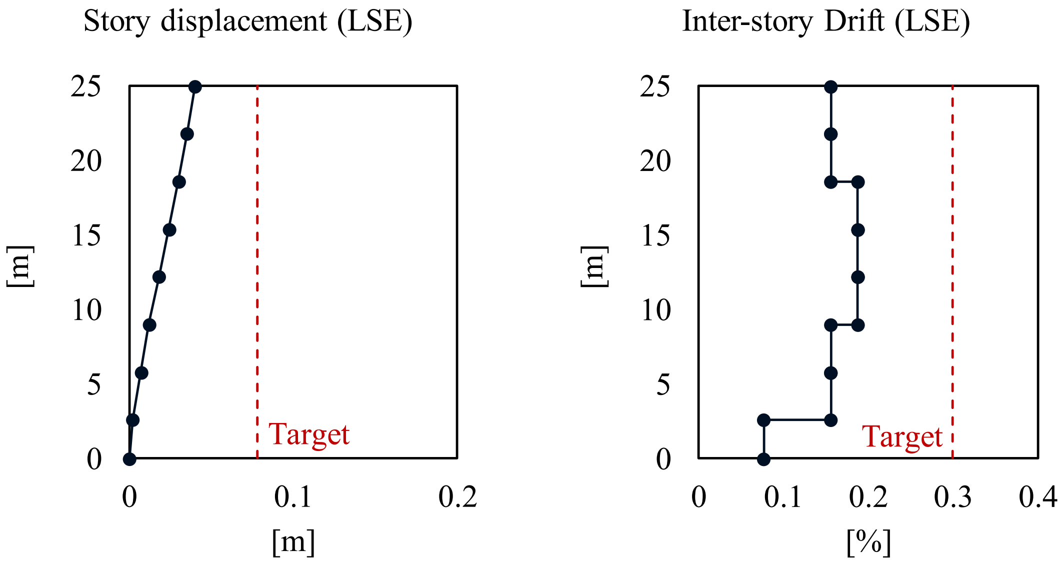

b) c)

Figure 16 a) Capacity curve of the retrofitted structure. Capacity curve of the whole system (black) and of the existing building (brown). b) story displacement and c) inter-story drift ratio at the Life Safety Earthquake (LSE).

To further assess the effectiveness of the retrofit, 7 non-linear time history analyses were also carried out. Accelerograms compatible with the code spectrum were determined by adopting the software Rexel 2.2beta [38]. A maximum average scale factor equal to 2 and upper and lower tolerances equal to 10% were imposed. The accelerogram identification codes (European Strong Motion Database [39]) and the relative scale factors are reported in *Table 5*.

Table 5 Selected combination of compatible ground motions (GM) used for the time history analyses *[38]*.

	Eq. id [39]	**Scale Factor**	**Station ID**	**Earthquake Name**	**Date**	**M_w**	**PGA_x [m/s^2]**	**PGA_y [m/s^2]**
GM 1	000170xa	3.0157	ST46	Basso Tirreno	15/04/1978	6	0.7188	1.5846
GM 2	000175ya	1.5158	ST50	Volvi	20/06/1978	6.2	1.3649	1.43
GM 3	000335ya	1.8432	ST121	Alkion	25/02/1981	6.3	1.1437	1.176
GM 4	000602ya	2.0323	ST224	Umbria Marche	26/09/1997	6	1.1441	1.0666
GM 5	000879ya	0.6924	ST271	Dinar	01/10/1995	6.4	2.6739	3.1306
GM 6	001708ya	2.1805	ST1253	Ano Liosia	07/09/1999	6	0.8158	0.9941
GM 7	007329xa	0.52607	ST87	Faial	09/07/1998	6.1	4.1204	3.749

Time history results, expressed in terms of maximum base shear of the whole system V_{MAX}, of the diagrid V'_{MAX}, and of the existing building V''_{MAX}, maximum axial force in the diagonals $N_{k,MAX}$, top displacement of the existing building d_{TOP}, and total drift of the existing building θ_{TOP}, are reported in *Table 6*.

Table 6 Time History results.

	V_{MAX} [kN]	V'_{MAX} [kN]	V''_{MAX} [kN]	$N_{k,MAX}$ [kN]	d_{TOP} [m]	θ_{TOP} [%]
Avg.	**8438.96**	**7001.33**	**1159.31**	**2371.71**	**0.058**	**0.23**
S.D.	**±1705.20**	**±1197.40**	**±3543.95**	**±525.16**	**±0.013**	**±0.05**

Results show that both the limit top displacement target of 0.074 m and the maximum inter-story drift target 0.3% are met.

In *Table 7*, the analytic predictions are compared with the average Finite Element Model results demonstrating the accuracy of the design method.

Table 7 Comparison of the analytic method and the FEM results.

	V_{MAX} [kN]	V'_{MAX} [kN]	V''_{MAX} [kN]	$N_{k,MAX}$ [kN]	d_{TOP} [m]	θ_{TOP} [%]
Avg. FEM (ES)	8438.96	7001.33	1159.31	2371.71	0.058	0.23
Analytic Method	7901.30	6264.80	1431.90	2545.50	0.056	0.22
Percentage error	-7%	-12%	+23%	+7%	-3%	-4%

The total base shear of the diagrid V_2= 7001.33 kN corresponds to a base shear flow of 200 kN/m and it is acceptable for the imposed limit of 250 kN/m. As for the story shear, the adopted limit value of 650 kN is exceeded in all the floors but 1st and 2nd (*Figure 17*), therefore, external diaphragms may be introduced. Such diaphragms can be designed considering the CPE and can be located in correspondence to the new external floors, therefore without requiring working from inside the building.

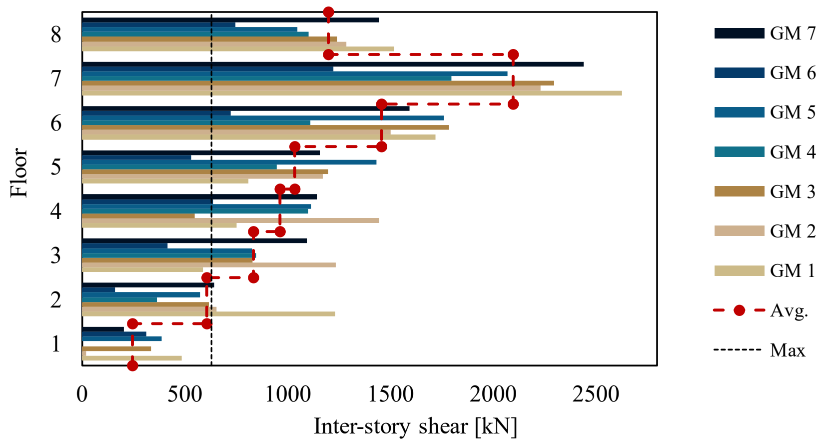

Figure 17 Floor shear along the building height.

In *Figure 18*a, the peak floor accelerations (PFAs) are plotted, and it can be seen that the maximum PFA occurs at the top floor levels. The mean values (red) of floor acceleration for the seven non-linear time histories have been observed to range between 0.1g and 0.7g. *Figure 19b* and *Figure 19c* show that both the story displacement and the inter-story drift target are met for all the considered accelerograms.

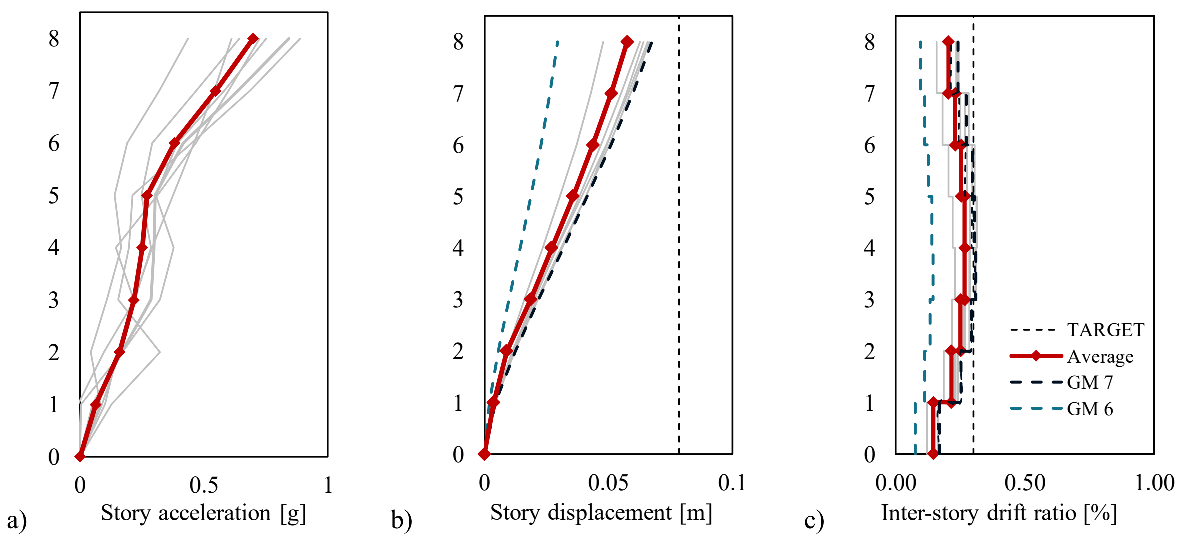

Figure 18 a) Peak Floor Acceleration, b) story displacement, c) inter-story drift.

Figure 19 shows the comparison between the numerical and analytical maximum forces in the diagonal elements at each floor. Results obtained from the simplified method slightly overestimate the axial forces in the diagonals, whilst the average stress rate of these elements is always smaller than the buckling limit. As expected, the average stress rate is particularly low at the upper floors.

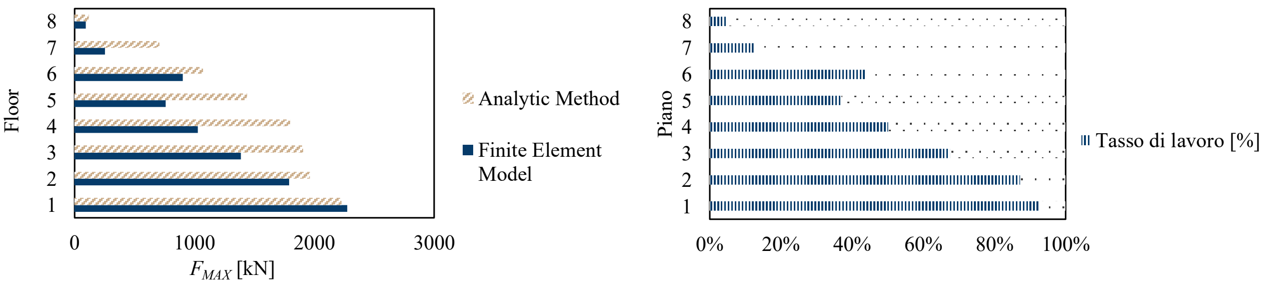

Figure 19 a) Comparison between the forces obtained from the analytical method and the FEM; b) stress rate of the most stressed diagonal at each floor.

Based on these results, a possible optimization of the elastic diagrid could be pursuit by reducing the cross-section area of the diagonal elements along the diagrid height as a function of the relative stress rate.

3.2.6 Behavior at collapse

As already introduced in *Section 2.4*, the behavior beyond the Life Safety Earthquake (LSE) must be controlled; for this reason, the capacity curve of 2 alternative retrofitted system are evaluated in *Figure 16a*: 1) an elastic solution (*grey*), 2) a non-linear solution in which a dissipative link is introduced in the diagonals at the base of the diagrid (*blue*).

In the first solution, the diagrid remains elastic also beyond the displacement demand related to the LSE. It can be observed that the new floor diaphragms must withstand substantial higher actions. In addition, the collapse of the retrofitted building is not associated with a ductile failure, and the new foundation system is overstressed.

In the second solution, some damage is allowed beyond the LSE at the ground floor of the existing building; however, a ductile behavior of the retrofitted building is guaranteed. By introducing a non-linear behavior, the maximum loads in the new floor diaphragms and in the new foundation system are respectful of the imposed design targets. In this case, the general links at the base of the diagrid were designed considering the compressive and tensile actions in the diagonal members calculated according to Equation 3.

4. Concluding remarks

This work is part of ongoing research on the holistic renovation of the post-World War II (WWII) Reinforced Concrete (RC) building stock, and it considers the adoption of diagrid exoskeletons as integrated retrofit solution. Diagrid exoskeletons may be conceived and designed in accordance to the Life Cycle

Thinking (LCT) principles [1], [16]. They can be assembled from outside and can be complemented with energy efficiency and architectural improvement measures. Given the high adaptability and flexibility of diagrids compared with other solutions, these structures can be easily adopted in incremental holistic rehabilitation plans when the initial costs of the retrofit are too high or the existing building functions cannot be relocated [8].

With the purpose of optimizing the structural performances of the retrofitted building and complying with the LCT principles, elastic over-resistant diagrids were investigated. Two different design proportioning methods were derived defining: 1) the geometry of the diagrid module, which depends on the layout of the existing building and on the optimization of the diagonals' inclination angle; 2) the diagrid stiffness, which must entail the reduction of the total inter-story drift to minimize damages induced by seismic events; 3) the minimum cross-section of the diagonal elements to avoid buckling.

In the first design method, the procedure developed for the design of diagrids for new tall buildings has been extended to be applied for the seismic retrofit of an existing building. Different load distributions were investigated and simplified static schemes were proposed. The results showed that a simplified configuration of the Timoshenko beam with triangular load distribution can be considered for buildings taller than 4 floors. Through the proposed Timoshenko beam model, preliminary proportioning of the diagrid exoskeletons and assessment of its effectiveness can be made. Given the high architectural potential and the high adaptability of diagrid structures, a preliminary evaluation of the dimension of diagonals and of the main diagrid features could be useful in the initial phase of the design procedure, also to evaluate the aesthetic impact of the diagrid on the existing building. Moreover, preliminary considerations about the seismic actions on the foundation system and on the existing floors can be made.

The second method is based on the definition of design spectra providing the minimum required elastic stiffness of the retrofit system as a function of the building characteristics. Starting from the considerations made by Ciampi et al. [15] on existing building equipped with dissipative bracings, sensitivity analyses on the retrofitted structure were conducted considering a simplified 2 DOF system representing the existing building and the retrofitting diagrid; basing on the results on these analyses, a set of design spectra are defined in order to simplify the design procedure and to derive the optimal retrofit parameters.

The effectiveness of both methods was assessed through the application to a reference building representative of ordinary 70s-80s RC European buildings.

It should be noted that when elastic and over-resistant systems are considered for the retrofit of RC infilled frames, the presence of very stiff elements with poor ductility (e.g. infills and staircase core) leads to stiff retrofit solutions and high seismic actions on the retrofitted building. In addition, following the substantial increment of seismic actions resulting from the stiffening of the building, a remarkable overload of floor diaphragms may occur after the retrofit. When the in-plane loads exceed the capacity of the floor, additional internal or external diaphragms may be required; the latter solution may be preferred anytime working from outside is an asset of the renovation project, as to minimize disruption of occupancy. In this paper, an upper bound in terms of maximum strength of the diagrid has been introduced to control the seismic action on the diaphragms, on the foundation system, and to guarantee a ductile behavior of the retrofitted building at collapse. In addition, providing a ductile behavior of the diagrid at the ground floor allows to lump damage in few elements in the case of exceptional events, thus reducing the impacts of the proposed solution in terms of costs and repair time.

Future research will focus on the analysis of other solutions for dissipative systems such as between the diagrid and the existing building as special connection elements [24] and on the adoption of responsive systems [37], i.e. structures capable to adapt their properties to the intensity of the earthquake [40]. Another research topic worth of investigation regards the evaluation of the stiffness and the strength of the connections between the diagrid and the existing building.

5. References

[1] A. Marini, C. Passoni and A. Belleri, "Life cycle perspective in RC building integrated renovation," in *XIV International Conference on Building Pathology and Constructions Repair – CINPAR*, Florence, 2018.

[2] S. Yadav and V. Garg, "Advantage of Steel Diagrid Building Over," *International Journal of Civil and Structural Engineering Research,* vol. 3, no. 1, pp. 394-406, 2015.

[3] K.-S. Moon, J. J. Connor and J. E. Fernandez, "Diagrid structural systems for tall buildings: characteristics and methodology for preliminary design," *The Structural Design of Tall and Special Buildings,* vol. 16, no. 2, pp. 205-230, 2007.

[4] BPIE, Europe's buildings under the microscope: A country-by-country review of the energy performance of the buildings, Brussel, 2011.

[5] I. Artola, K. Rademaekers, R. Williams and J. Yearwood, "Boosting Building Renovation: What potential and value for Europe?," Policy Department A: Economic and Scientific Policy - European Parliament, Brussels, 2016.

[6] F. Krimgold, D. Hattis and M. Green, Incremental seismic rehabilitation of multifamily apartment buildings: providing protection to people and buildings, Washington, D.C.: U.S. Dept. of Homeland Security, FEMA, 2004.

[7] P. La Greca and G. Margani, "Seismic and Energy Renovation Measures for Sustainable Cities: A Critical Analysis of the Italian Scenario," *Sustainability,* vol. 10, no. 1, p. 254, 2018.

[8] J. Zanni, S. Labò, C. Passoni, E. Casprini, A. Marini, A. Belleri and M. Costantino, "Incremental Integrated Holistic Rehabilitation: a new concept to boost a deep renovation of the existing building stock," Prague, 2019.

[9] A. Marini, C. Passoni, A. Belleri, F. Feroldi, M. Preti, G. Metelli, P. Riva, E. Giuriani and G. Plizzari, "Combining seismic retrofit with energy refurbishment for the sustainable renovation of RC buildings: a proof of concept," *European Journal of Environmental and Civil Engineering,* pp. 1-21, 2017.

[10] K.-S. Moon, "Practical Design Guidelines for Steel Diagrid Structures," *Aei 2008,* 2008.

[11] E. Mele, M. Fraldi, G. M. Montuori and G. Perrella, "Non-conventional Structural Patterns for Tall Buildings: from Diagrid to Hexagrid and Beyond," in *Fifth International Workshop on Design in Civil and Environmental Engineering*, Rome, 2016.

[12] E. Mele, M. Toreno, G. Brandonisio and A. De Luca, "Diagrid structures for tall buildings: case studies and design considerations," *The Structural Design of Tall and Special Buildings,* vol. 23, no. 2, pp. 124-145, 2012.

[13] G. M. Montuori, E. Mele, G. Brandonisio and A. De Luca, "Design criteria for diagrid tall buildings: Stiffness versus strength," *The Structural Design of Tall and Special Buildings,* vol. 23, no. 17, pp. 1294-1314, 2013.

[14] G. M. Montuori, M. Fadda, G. Perrella and E. Mele, "Hexagrid - hexagonal tube structures for tall buildings: patterns, modeling, and design," *The Structural Design of Tall and Special Buildings,* vol. 24, no. 15, pp. 912-949, 2015.

[15] V. Ciampi, M. De Angelis and F. Paolacci, "Design of yielding or friction-based dissipative bracings for seismic protection of buildings," *Engineering Structures,* vol. 17, no. 5, pp. 381-391, 1995.

[16] C. Passoni, S. Labò, A. Marini, A. Belleri and P. Riva, "Renovating the existing building sotck: a life cycle thinking desing approach," in *16th European Conference on Earthquake Engineering - ECEE*, Thessaloniki, 2018.

[17] I. Almufti and M. Willford, "The REDi™ rating system: A framework to implement resilience-based earthquake design for new buildings," in *10th U.S. National Conference on Earthquake Engineering: Frontiers of Earthquake Engineering.*, NCEE, 2014.

[18] EC8, *Design of structures for earthquake resistance,* Brussels, Belgium: European Committee for Standardization, CEN 2005.

[19] W. F. Baker, Structural possibilities. In: Parker D, Wood A (eds.) The tall buildings reference book, London: Routledge Taylor & Francis Group, 2013.

[20] M. R. Maqhareh, "The Evolutionary Process of Diagrid Structure Towards Architectural, Structural and Sustainability Concepts: Reviewing Case Studies," *Journal of Architectural Engineering Technology,* vol. 3, no. 2, 2014.

[21] D. Cardone and G. Perrone, "Damage and Loss Assessment of Pre-70 RC Frame Buildings with FEMA P-58," *Journal of Earthquake Engineering,* vol. 21, no. 1, pp. 23-61, 2017.

[22] S. Labò, *Holistic sustainable renovation of Post-World War II reinforced concrete building under a life cycle perspective by means diagrid exoskeletons. (PhD thesis),* University of Bergamo, 2019.

[23] F. Feroldi, *Sustainable renewal of the post WWII building stock through engineered double skin, allowing fro structural retrofit, energy efficiency upgrade, architectural restyling and urban regeneration. (PhD Thesis),* University of Brescia, 2014.

[24] S. Labò, C. Passoni, A. Marini, A. Belleri and P. Riva, "Design spectra for the preliminary design of elastic seismic retrofit solution from the outside," in *7th ECCOMAS Thematic Conference on Computational Methods in Structural Dynamics and Earthquake Engineering - COMPDYN*, Crete, 2019.

[25] A. Marini, C. Passoni, P. Riva, P. Negro, R. Elvira and F. Taucer, Technology option for earthquake resistant, eco-efficient buildings in Europe: Research needs, Publications Office of the European Union, 2014.

[26] IDES, "Verifiche tecniche dei livelli di sicurezza sismica ai sensi dell'O.P.C.M. N.3274/2003 e S.M.I. dell'edificio "H" del quartiere Chiesanuova di proprietà dell'ALER - Azienda Lombarda per l'Edilizia Residenziale di Brescia," Brescia, 2008.

[27] M. Zanchi and L. Vassalli, *Pratiche di riqualificazione integrata: applicazione ad un edificio ALER di social housing (Degree thesis),* University of Bergamo, 2016.

[28] MidasGEN, "Analysis Manual for Midas GEN," 2018.

[29] S. Otani, *SAKE: A Computer Program for Inelastic Response of R/C Frames to Earthquakes,* 1974.

[30] D. Bull, "Understanding the Complexities of Designing Diaphragms in Buildings for Earthquakes," *Bulletin of New Zealand Society for Earthquake Engineering,* vol. 37, no. 2, pp. 70-88, 2004.

[31] A. Marini, A. Belleri, C. Passoni, F. Feroldi and E. Giuriani, "In-plane diaphragm action in existing beam and block floor systems," *Engineering Structures,* 2019.

[32] F. Feroldi, A. Belleri, A. Marini, C. Passoni and E. Giuriani, "Il ruolo critico dei diaframmi di piano negli interventi di adeguamento sismico condotti dall'esterno," in Proceedings of XVIII ANIDIS congress, Ascoli Piceno, 15-19 settembre 2019. DOI: 10.1400/271066.

[33] L. Decanini, C. Gavarini and S. Bertoldi, "Telai tamponati soggetti ad azioni sismiche, un modello semplificato: confronto sperimentale e numerico," in *VI Convegno Nazionale di Ingegneria Sismica in Italia*, Perugia, 1993.

[34] A. B. Mehrabi, B. P.-S. Shing, M. P. Schuller and J. L. Noland, "Experimental evaluation of masonry-infilled RC frames," *Journal of Structural Engineering,* vol. 122, no. 3, pp. 228-237, 1996.

[35] NTC, *Norme Tecniche per le Costruzioni (NTC 2018),* Gazzetta Ufficiale del 20/02/2018, Supplemento ordinario n.42, 2018.

[36] P. Fajfar, "A Nonlinear Analysis Method for Performance-Based Seismic Design," *Earthquake Spectra,* vol. 16, no. 3, pp. 573-592, 2000.

[37] C. Passoni, *Holistic renovation of existing RC buildings: a framework for possible integrated structural interventions. (PhD thesis),* University of Brescia, 2016.

[38] I. Iervolino, C. Galasso and E. Cosenza, "REXEL: computer aided record selection for code-based seismic structural analysis," *Bulletin of Earthquake Engineering,* vol. 8, pp. 339-362, 2010.

[39] N. N. Ambraseys, P. Smit, J. Douglas, B. Margaris, R. Sigbjornsson, S. Olafsson, P. Suhadolc and G. Costa, "Internet site for European strong-motion data," *Bollettino di Geofisica Teorica ed Applicata,* vol. 45, no. 3, pp. 113-129, 2004.

[40] S. Labò, C. Passoni, A. Marini, A. Belleri, G. Camata, P. Riva and E. Spacone, "Prefabricated responsive diagrids for holistic renovatin of existing mid-rise RC buildings," in *6th ECCOMAS Thematic Conference on Computational Methods in Structural Dynamics and Earthquake Engineering - COMPDYN*, Rhodes, 2017.

Appendix A: Design Spectra

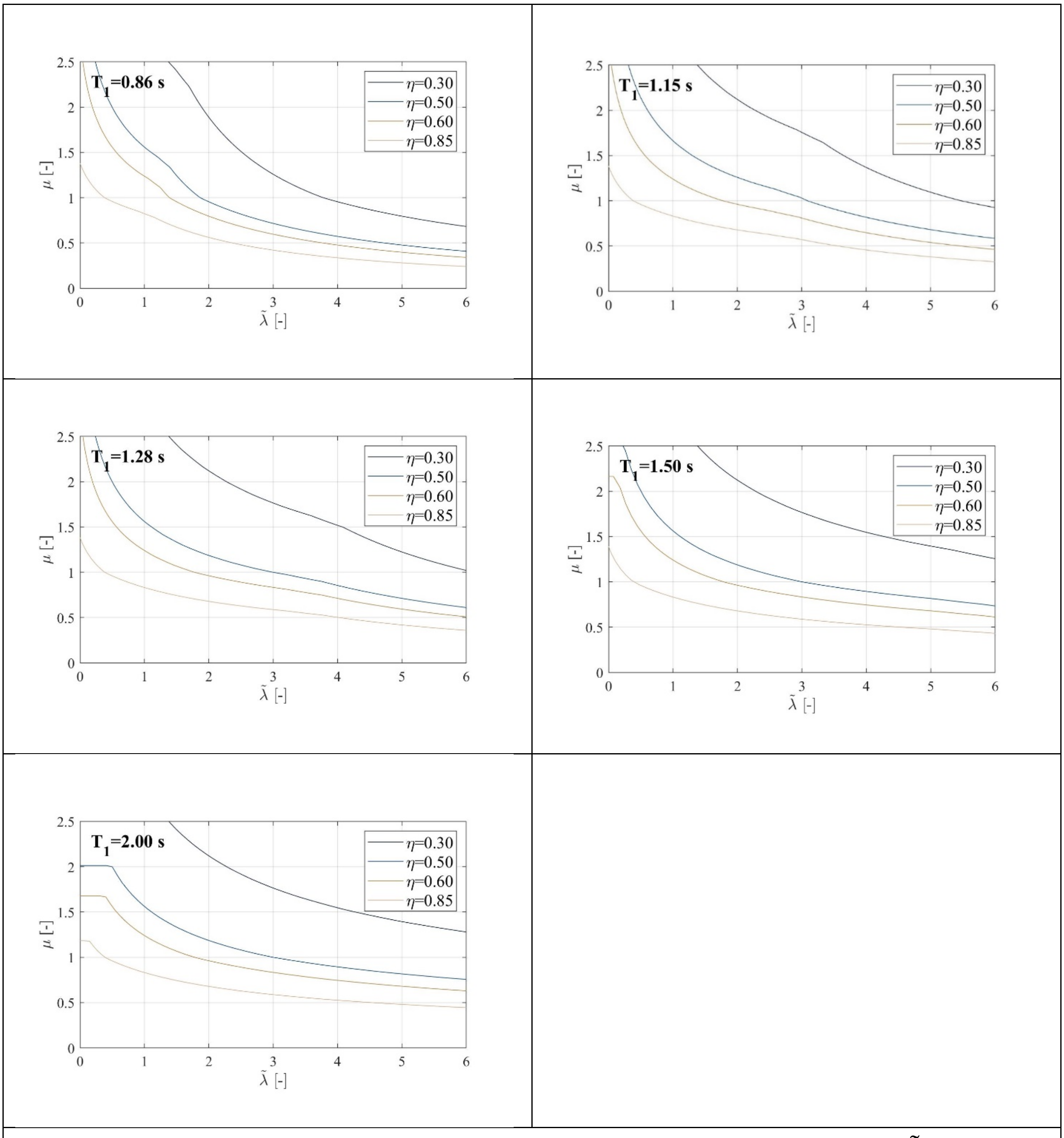

Figure A1 Ductility demand (μ) on the existing building as a function of the retrofit stiffness ratio ($\tilde{\lambda}$) for varying adimensionalized yielding force (η) and fundamental period (T_1) of the existing building.

Appendix B: Geometry and steel rebars

Columns

Ground Floor			
Column	*Lx [cm]*	*Ly [cm]*	*Steel rebars*
31	30	40	4Φ14+ 2 Φ12
32, 35, 36, 46, 49, 52	30	60	6Φ16
33, 38-40, 43-45, 53	30	50	6Φ14
34, 35, 47, 48, 50, 51	45	30	6Φ14
54, 55	30	35	4Φ14+ 2 Φ12

First Floor			
Column	*Lx [cm]*	*Ly [cm]*	*Steel rebars*
31	30	35	4Φ14+ 2 Φ10
32, 35, 36, 41 ,45, 46, 49, 52	30	50	6Φ14
33,34,38 -40, 43-45	30	40	4Φ14+ 2 Φ12
34	40	30	4Φ14+ 2 Φ12
55	30	30	6Φ14

Second Floor			
Column	*Lx [cm]*	*Ly [cm]*	*Steel rebars*
31	30	30	4Φ14
32	30	40	4Φ14+2Φ12
33	30	35	4Φ14+2Φ10
34	35	30	4Φ14+2Φ10
55	30	30	4Φ14

Third Floor			
Column	*Lx [cm]*	*Ly [cm]*	*Steel rebars*
31,33,34,38-40,43-45,47,50,51,53-55	30	30	4Φ14
32,35,36,41,46,49,52	30	35	4Φ14+2Φ10

Fourth-Fifth-Sixth-Seventh-Eighth Floors			
Column	*Lx [cm]*	*Ly [cm]*	*Steel rebars*
31-55	30	30	4Φ14

Stirrups Φ6/20

Columns

Floors from 1 to 7		Middle			Support		
Columns	*Base [cm]*	*Height [cm]*	*Stirrup*	*Steel rebars (Top)*	*Steel rebars (Bottom)*	*Steel rebars (Top)*	*Steel rebars (Bottom)*
53-50, 54-51	30	42	Φ6/20	4Φ12	2Φ10	2Φ12	2Φ10+2Φ12
45-48, 50-47, 51-48	30	42	Φ6/20	2Φ10+2Φ12	2Φ10	2Φ12	4Φ10
47-44, 34-31	30	42	Φ6/20	2Φ12+2Φ14	2Φ10	2Φ12	2Φ10+2Φ14
44-41	30	42	Φ6/20	3Φ12	2Φ10	2Φ12	2Φ10+1Φ12
41-39	30	42	Φ6/20	2Φ14	2Φ14	2Φ14	2Φ14
52-53	30	42	Φ6/20	4Φ10	2Φ10	2Φ10	4Φ10
52-55, 45-Wall, Wall-34	30	42	Φ6/20	4Φ12	2Φ10	2Φ12	2Φ10+2Φ12
54-55	30	42	Φ6/20	2Φ10+2Φ12	2Φ10	2Φ10	2Φ10+2Φ12
31-32	30	42	Φ6/20	2Φ10+2Φ12	2Φ10	2Φ10	2Φ10+2Φ12
32-33	30	42	Φ6/20	4Φ10	2Φ10	2Φ10	4Φ10
35-38, 46-43	70	22	Φ8/20	7Φ12	3Φ10	3Φ12	4Φ12+3Φ10
38-40, 43-40	70	22	Φ8/20	4Φ12	3Φ10	3Φ12	3Φ10+1Φ12
52-49	80	22	2Φ8/20	2Φ10+6Φ12+2Φ14	4Φ10	2Φ10+4Φ12	4Φ10+2Φ12+2Φ14
49-46	80	22	2Φ8/20	8Φ12+2Φ10	4Φ10	4Φ10+2Φ12	4Φ10+4Φ12
35-35	90	22	2Φ8/20	4Φ12+4Φ14	4Φ10	4Φ10+4Φ14	4Φ12
39-36	90	22	2Φ8/20	8Φ12	4Φ10	4Φ10+4Φ12	4Φ12
36-33	90	22	2Φ8/20	4Φ12+4Φ14	4Φ10	4Φ12	4Φ10+4Φ14
31-34, 34-Wall, 48-51, 53-50, 41-44, 31-32, 32-33, 51-52, 52-53	30	42	Φ6/20	2Φ12	2Φ12	2Φ12	2Φ12
47-50, 44-47	30	42	Φ6/20	2Φ12+2Φ14	2Φ12	2Φ12	2Φ12+2Φ14
49-52, 46-49	50	22	Φ6/15	3Φ12+2Φ14	3Φ10	3Φ12	3Φ10+2Φ14
43-46	50	22	Φ6/15	3Φ12+2Φ14	3Φ10	3Φ12	3Φ10+2Φ14
40-43	50	22	Φ6/15	3Φ12	3Φ10	3Φ12	3Φ10
38-40	50	22	Φ6/15	2Φ12+1Φ14	3Φ10	2Φ12+1Φ14	3Φ10
32-35	50	22	Φ6/15	2Φ12+3Φ14	3Φ10	2Φ12+1Φ14	3Φ10+2Φ14
35-38	50	22	Φ6/15	4Φ12+1Φ14	3Φ10	2Φ12+1Φ14	3Φ10+2Φ12
Wall-45, 45-48	30	30	Φ6/20	2Φ10	2Φ10	2Φ10	2Φ10
33-36	40	22	Φ6/15	2Φ12+2Φ14	2Φ12	2Φ12	2Φ12+2Φ14
36-39	40	22	Φ6/15	4Φ12	2Φ12	2Φ12	4Φ12
39-41	40	22	Φ6/15	2Φ12	2Φ12	2Φ12	2Φ12
31-34	30	42	Φ6/20	2Φ12	2Φ12	2Φ12	2Φ12
32-35	30	35-40	Φ8/20	4Φ12	3Φ10	2Φ12	3Φ10+2Φ12
35-38	30	35-40	Φ8/20	2Φ10+2Φ12	3Φ10	2Φ12	5Φ10
38-40, 40-43	30	35-40	Φ8/20	2Φ12	2Φ10	2Φ12	2Φ10
43-46, 46-49	30	35-40	Φ8/20	4Φ10	3Φ8	2Φ10	3Φ8+2Φ10
49-52	30	35-40	Φ8/20	2Φ10+2Φ8	3Φ8	2Φ10	5Φ8
33-36	30	40-51	Φ8/20	2Φ10+2Φ12	2Φ10	2Φ10	2Φ10+2Φ12
36-39	30	40-51	Φ8/20	4Φ10	2Φ10	2Φ10	4Φ10
39-41	30	40-51	Φ8/20	2Φ10	2Φ10	2Φ10	2Φ10
41-44	30	40-51	Φ8/20	2Φ10+2Φ14	2Φ10	2Φ12	2Φ10+2Φ14
31-34	30	30-41	Φ8/20	2Φ12+2Φ14	2Φ10	2Φ12	2Φ10+2Φ14
34-Wall, 48-51	30	30-41	Φ8/20	4Φ12	2Φ10	2Φ12	2Φ10+2Φ12
Wall-45	40	20	Φ8/20	2Φ12+2Φ14	2Φ12	2Φ12	2Φ12+2Φ14
45-48	40	20	Φ8/20	2Φ12+2Φ14	2Φ12	2Φ12	2Φ12+2Φ14
31-32, 32-33, 51-52	30	20	Φ6/25	2Φ10	3Φ8	2Φ10	3Φ8
52-53, 46-47, 49-50, 43-44	20	50	Φ6/20	2Φ10+2Φ14	2Φ10	2Φ14	4Φ10
32-35	30	35-40	Φ8/20	4Φ12	3Φ10	2Φ12	3Φ10+2Φ12

List of symbols

$\tilde{k}$	Equivalent stiffness of the SDOF system
$\tilde{c}$	Equivalent damping of the SDOF system
$\hat{k}$	Total stiffness of the SDOF system
$\tilde{\lambda}$	Stiffness ratio: $\tilde{k} / k_1$
$A_{d,f}$	Cross-section area of the diagonal elements on the "flange"
$A_{d,w}$	Cross-section area of the diagonal elements on the "web"
$A_d^{stiffness}$	Cross-section area of the diagonal element obtained with the stiffness-based design
$A_d^{strength}$	Cross-section area of the diagonal element obtained with the strength-based design
$a_{floor,max}$	Maximum floor acceleration
A_s	Cross-section area of the diagonal elements
c_1	Damping coefficient of the DOF1
c_{12}	Damping coefficient of the DOF2
c_2	Damping coefficient of the connection
D	Distance of the *i-th* module from the whole diagrid centroid axis
d_k	Distance of the *k-th* module from the whole diagrid centroid axis
d_{TOP}	Target maximum top displacement of the existing building
E	Elastic modulus of the diagonal element
$F_{m,k}$	Forces in the *k-th* module due to overturning moment
$F_{p,k}$	Forces in the *k-th* module due to vertical loads
$F_{v,k}$	Forces in the *k-th* module due to shear force
$F_{y,1}$	Yielding force of the DOF1
f_{yk}	Maximum allowed axial stress allowed
G	Shear modulus
H	Existing building height
h_i	Inter-story height
I	Area moment of inertia of the diagonal elements
k	Timoshenko shear coefficient
k_1	Initial elastic stiffness of the DOF1
k_{12}	Initial elastic stiffness of the connection
k_2	Initial elastic stiffness of the DOF2
l	Plan direction of the building parallel to the considered horizontal loads direction
L_d	Diagonal elements length
M	Bending Moment
m^*	Mass of the equivalent SODF system
m_1	Effective mass of the DOF1
m_2	Effective mass of the DOF2
n	Number of floors of the existing building
n_f	Number of diagonals on the "flange" façade
N_k	Axial force in the diagonal element
n_k	Total number of the modules in the whole diagrid
N_k^{LIM}	Maximum allowed axial stress
$N_{m,k}$	Internal actions due to overturning moment
$N_{p,k},$	Internal actions due to vertical loads
$N_{v,k}$	Internal actions due to shear force
n_w	Number of diagonals on the "web" façade
n_X, n_Y	Principal directions
p	Triangular distributed load
$q_{foundation,max}$	Existing foundation capacity
S_a^D	Design spectrum acceleration
S_d^D	Design spectrum displacement
$s_{stiffness}$, $s_{srength}$	Tubular thickness obtained with the stiffness and strength method

T_1	Elastic period of the DOF1
u_1	Displacement of the DOF1
V	Shear action
$V_{floor,max}$	Floor diaphragm capacity
$V_{staircase,max}$	Maximum shear action in existing staircase walls
X_g	Ground acceleration
$y(x)$	Displacement of the Timoshenko beam in the variable x
α	Angle between the lateral load direction and the web façade
$\delta_{y,1}$	Yielding displacement of the bi-linear curve of the existing building
$\Phi_{stiffenss}$, $\Phi_{strength}$	Diameter of the diagonal elements obtained with the stiffness and strength method
χ	Coefficient functions of the profile slenderness
δ_{MAX}	Maximum displacement experienced by the DOF 1
γ_{M0}	Material safety factor
η	Yield force adimensionalized with respect to the mass (m_1) multiplied by the ground acceleration ($Sa(T_1)$)
λ	Stiffness ratio: k_2/k_1
μ^R	Ductility demand for the Reference case
μ	Ductility demand
θ	Inter-story drift ratio target
θ_{TOP}	Total drift of the existing building
ξ	Shear deformation
ψ	Diagonal element inclination